Improving the Efficiency of Gas Engines using Pre-chamber Ignition

Shah, Ashish

2015

Improving the Efficiency of Gas Engines using Pre-chamber Ignition

Doctoral Thesis

(Electronic version)

Ashish Shah
Division of Combustion Engines
Department of Energy Sciences

Sweden, December 2015

LUND
UNIVERSITY

ISBN 978-91-7623-561-4 (printed version)
978-91-7623-562-1 (electronic version)
ISRN LUTMDN/TMHP-15/1113-SE
ISSN 0282-1990

Division of Combustion Engines
Department of Energy Sciences
Faculty of Engineering
Lund University
P.O. Box 118
SE-221 00 Lund
Sweden

Abstract

The aim of this project is to explore and understand the combustion phenomenon in engines operating on gaseous fuels, and develop technologies as an alternative to the present diesel engine technologies for heavy duty applications; which are facing severe challenges like stringent emissions norms, high technology costs and unsustainable fuel supply. The studies presented in this thesis focus on the application of pre-chamber ignition system in heavy duty natural gas engines, as a means to improve fuel efficiency and reduce NO_x emissions.

Initial experiments using pre-chamber spark plugs without auxiliary fueling showed improvements in combustion stability, but with only a marginal extension in the dilution limit with excess air and EGR; and hence no significant fuel efficiency improvements. Following these observations, a literature survey was conducted and it was soon realized that additional fueling to the pre-chamber will help scavenge the pre-chamber at the beginning of every cycle and also lead to the formation of an easily combustible mixture inside the pre-chamber, even while the main chamber is extremely fuel-lean. Further experiments conducted on a single cylinder engine with a custom made pre-chamber assembly with auxiliary fueling showed considerable extension of the dilution limit of main chamber combustion, from an excess air ratio (λ) of about 1.7 (with an un-fueled pre-chamber) to over 2.6. The maximum indicated efficiency observed at an operating load of 10 bar $IMEP_g$ was over 47% with engine-out NO_x emission levels below the 'EURO 6' limits (for heavy duty natural gas engines).

Following these finding, experiments to study the effect of pre-chamber volume and nozzle diameter on resulting main chamber ignition were conducted, where the pre-chamber volume fraction of 2.4% and the nozzle diameter ratio in the range of 0.025-0.035 cm^{-1} were found to be optimum. CFD simulations were then conducted to understand the fluid dynamic aspects of interactions between the pre-chamber jets and the main chamber charge, which revealed the importance of jet momentum and jets-wall interaction on main chamber ignition. Further experiments on a large bore marine engine to understand scaling requirements for pre-chamber design showed that the optimal pre-chamber volume (and with it the nozzle diameter) scales with the displacement volume of the engine. Gross indicated efficiency of 50% was also recorded.

Thesis contributions

The main contribution of the research presented in this thesis is the *proof of concept* for a pre-chamber ignition system operating with fuel rich pre-chamber combustion strategy as a very effective alternative ignition system for heavy duty natural gas engines. The studies also contribute to the fundamental knowledge and understanding of the mechanism of pre-chamber ignition. The main contribution are listed below:

- It has been demonstrated that a pre-chamber ignition system without auxiliary fueling improves combustion stability and main chamber ignition, but is not capable of considerably extending the dilution limit of main chamber combustion.
- It has been demonstrated that a pre-chamber ignition system with auxiliary fueling, and specifically when a fuel-rich mixture is formed inside the pre-chamber, can substantially extend the dilution limit of main chamber combustion, such that a considerable improvement in fuel efficiency is achieved.
- The optimal pre-chamber volume of 2.4% of the engine's compression volume and a nozzle diameter ratio of 0.025-0.035 cm^{-1} are proposed, for an optimal trade-off between main chamber ignition characteristics and engine out NO_x emissions.
- It has been shown that with an optimized pre-chamber ignition system, a heavy duty natural gas engine can operate with 50% gross indicated efficiency, an improvement from 42% with a conventional spark plug ignition system.

List of Publications

This thesis is based on the following papers, which will be referred to in the text by their Roman numerals.

I Shah, A., Tunestal, P., and Johansson, B., *"Investigation of Performance and Emission Characteristics of a Heavy Duty Natural Gas Engine Operated with Pre-Chamber Spark Plug and Dilution with Excess Air and EGR,"* SAE Int. J. Engines 5(4):1790-1801, 2012.

II Shah, A., Tunestal, P., and Johansson, B., *"Applicability of Ionization Current Sensing Technique with Plasma Jet Ignition Using Pre-Chamber Spark Plug in a Heavy Duty Natural Gas Engine,"* SAE Technical Paper 2012-01-1632, 2012.

III Shah, A., Tunestal, P., and Johansson, B., *"Effect of Relative Mixture Strength on Performance of Divided Chamber Avalanche Activated Combustion Ignition Technique in a Heavy Duty Natural Gas Engine,"* SAE Technical Paper 2014-01-1327, 2014.

IV Shah, A., Tunestal, P., and Johansson, B., *"Effect of Pre-Chamber Volume and Nozzle Diameter on Pre-Chamber Ignition in Heavy Duty Natural Gas Engines,"* SAE Technical Paper 2015-01-0867, 2015.

V Shah, A., Tunestal, P., and Johansson, B., *"CFD Simulations of Pre-chamber Jets' Mixing Characteristics in a Heavy Duty Natural Gas Engine,"* SAE Technical Paper 2015-01-1890, 2015.

VI Shah, A., Tunestal, P., and Johansson, B., *"Scalability aspects of Pre-chamber Ignition in Heavy Duty Natural Gas Engines,"* SAE Technical Paper, 2016.

Manuscript submitted for publication and presentation at the SAE 2016 World Congress and Exhibition, April 12-14, 2016 at Detroit, Michigan, USA.

Acknowledgements

First of all, I would like to express my gratitude to my main supervisor, Prof. Per Tunestål for all the guidance and support throughout my doctoral studies. I have always been impressed by his multi-faced knowledge, which spans well beyond the field of combustion engines! His friendliness and down-to-earth nature always made me feel comfortable in any situation.

I am equally thankful to Prof. Bengt Johansson who was my co-supervisor and also the head of the division of combustion engines. His fundamental and applied knowledge of combustion engines is unrivaled! Conversations with him always included his witty remarks which made even the most complex discussions fun filled! Bengt also deserves a special thanks because he was my first point of contact with this division (in fact with Sweden) when I as a complete stranger met him in India back in 2011 and said *"I want to do a Ph.D at your division at Lund University"*, and he was kind enough to grant my wish and make everything upto this thesis possible. *Thank you!*

I am also thankful to Prof. Öivind Andersson and Dr. Martin Tunér at our division for their friendly attitude and discussions with me. With four such seniors and their knowledge and expertize at the division, I seldom felt the need to consult a technical or a language dictionary!

My research consisted of extensive laboratory work with engines and none of my accomplishments in the lab would have been possible without the laboratory technicians. All of them have been a great source of help and practical learning. I am specifically thankful to Tommy Petersen, Mats Bengtsson, Kjell Jonholm, Viktor Atanasovski, Patrik Johansson and Thomas Johansson.

I would also like to thank my project's reference group members - Ola Stenlåås from Scania, Ingemar Magnusson from Volvo and Jari Hyvönen and Sebastiaan Bleuanus from Wärtsilä for their valuable technical feedbacks and also assessing the industrial relevance of my research.

Any way of expressing gratitude to my friends and fellow students will be an understatement! The time and fun shared with them has always helped me relieve my stress and at time frustration due to the lab where something was always *not working!* A special thanks to my friends with whom I have shared my office – Hadeel Solaka, Nhut Lam, Sam Shamun, Erik Svensson and Changle Li, for the fun times and also bear with my silly baseless jokes! I am equally thankful to Prakash Narayanan, Srikanth Deshpande, Atanu Kundu, Yann Gallo, Jessica Dahlström and Mengqin Shen for their good friendship and fun memories!

Last but not the least, I would like to thank my entire family for their love, support and understanding throughout the duration of my doctoral studies.

Abbreviations and Symbols

AFR	Air to fuel ratio (% m/m)
aTDC	After the firing top dead center
BDC	Bottom dead center
bTDC	Before the firing top dead center
CAD	Crank angle degree
CFD	Computational fluid dynamics
CH_4	Methane
CNG	Compressed natural gas
CO	Carbon monoxide
COV	Coefficient of variation
C.SP	Conventional spark plug
CO_2	Carbon dioxide
EGR	Exhaust gas recirculation
GHG	Green house gases
GWP	Global warming potential
H_2O	Water
IMEP	Indicated mean effective pressure
LHV	Lower heating value
MC	Main chamber
NMHC	Non-methane hydrocarbon
NO_x	Oxides of Nitrogen
PC	Pre-chamber
PC.SP	Pre-chamber spark plug
PM	Particulate matter
RANS	Reynolds-averaged NavierStokes
TDC	Top dead center
THC / HC	Total hydrocarbon
λ, α	Excess air ratio

Contents

Chapter 1

Introduction

The modern society is heavily dependent on its transportation systems, which are useful not only for personal mobility, but also for the transport of various goods and services which have become an integral part of our lives. The transportation system can therefore be considered as the back-bone of the socio-economic system that exists today and a life without it is unimaginable. But as much a boon it is to the society, it also poses several threats like energy security concerns for a country, adverse effect on human health and to the climate. This chapter begins by briefly discussing the challenges currently faced by countries in operating a sustainable and environmentally benign transportation system. The potential of natural gas as an alternative fuel to address some of the challenges is then discussed, and finally, the hurdles faced in successfully implementing such alternative solutions are presented, which also motivates the research presented in this thesis.

1.1 Challenges in the Transportation System

The two main challenges in today's transportation system are its effect on the climate and human health, and the concern of energy security at a national level.

Recently published data [1] plotted in figure 1.1 shows that the global emissions of Green House Gases (GHG) are increasing and that one of the main reasons is the emission of CO_2 due to combustion of fossil fuels. It can also be seen that the transport sector is one of the major contributors with 13.1% of total GHG emissions. Data from well developed regions of the world, such as the European Union [2] and the United States of America [3], show that the contribution of the transport sector to their total GHG emissions is well over 25% since other sectors like power generation are comparatively environmentally benign. Within the transport sector, the main contributor is the internal combustion engine which produces carbon-dioxide (CO_2), water vapor (H_2O), nitric oxide and methane (CH_4), all of which are known green house gases.

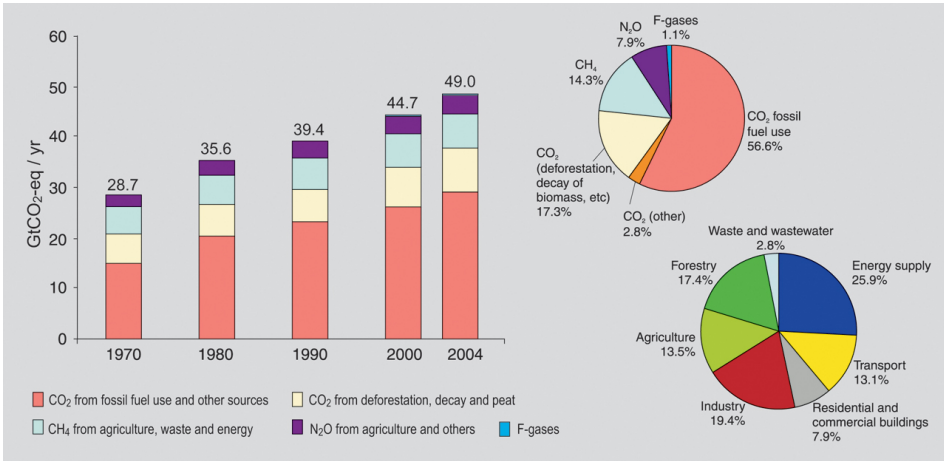

Figure 1.1: Global CO_2 emissions and the contribution of the transportation system [1]

This increased concentration of GHGs in the Earth's atmosphere acts like a *blanket* by preventing the loss of energy to outer space and making the planet warmer than it would otherwise be. This hypothesis, generally refereed to as the Green House Effect, is supported by recorded historical data on global average temperatures and the resulting after-effects on loss of ice cover near the poles and global average sea level rise, as can be seen in Figure 1.2. These effects are believed [2] to be the cause of increased rate of natural calamities, changing weather patterns and longer 'warm periods' observed through-out the world in the previous century.

In addition to these global consequences, internal combustion engines also pose local threats because other gases and particles released due to combustion are harmful to human health. Oxides of Nitrogen (NO_x) contributes to the formation of ground-level ozone, reacts to form nitrate particles, acid aerosols, as well as NO_2; all of which cause serious respiratory problems [4]. Unburnt hydrocarbon (HC) emissions, which are generally classified as methane (CH_4) and non-methane hydrocarbons (NMHC), are, apart from being GHGs, harmful to humans as they cause eye, nose, and throat irritation; headaches, loss of coordination, nausea; damage to liver, kidney, and the central nervous system [5]. Emissions of Carbon-monoxide (CO) are extremely harmful because Carbon monoxide poisoning is the most common type of fatal air poisoning in many countries [6]. Carbon monoxide is colorless, odorless, and tasteless, but highly toxic. It combines with hemoglobin to produce carboxyhemoglobin, which usurps the space in hemoglobin that normally carries oxygen, but is ineffective for delivering oxygen to bodily tissues. Concentrations as low as 667 ppm (0.0667%) may cause up to 50% of the body's hemoglobin to convert to carboxyhemoglobin [7] which may result in seizure, coma,

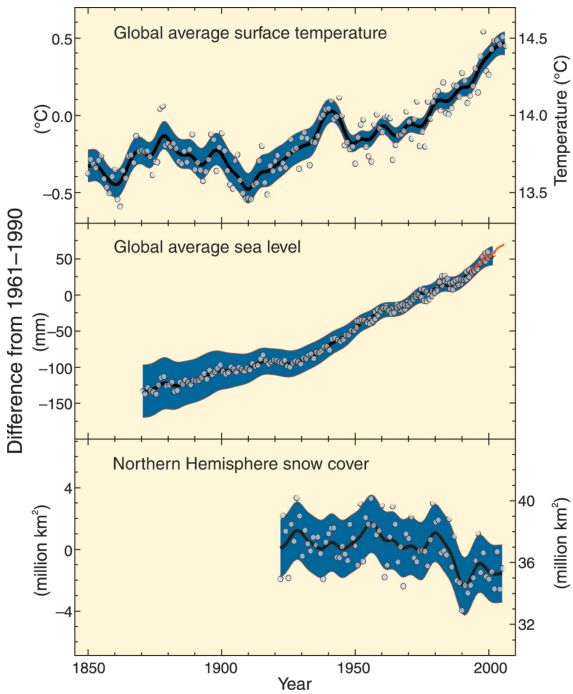

Figure 1.2: Historical data on average surface temperatures, ice cover at the poles and global sea levels [1]

and fatality. Another type of emissions from internal combustion engines are particulate matter (PM). The effects of inhaling particulate matter in humans and animals include asthma, lung cancer, cardiovascular disease, respiratory diseases, premature delivery, birth defects, and premature death [8]. Soot (a type of particulate matter) emitted largely from diesel engines, which was previously classified as probably carcinogenic to humans in 1988, was, in 2012, reclassified as carcinogenic to humans (group 1) by the International Agency for Research on Cancer (IARC) under the World Health Organization [9].

Another important challenge of today's transportation system is that of energy security because many countries are heavily dependent on import of oil for their mobility and transportation needs. For example, for the year 2010 in Europe, oil accounted for 94% of energy consumed in transport out of which 84% was imported with a bill of up to €1 billion a day [10]. Most of the oil supply in the world comes from politically unstable countries in the middle east (Figure 1.3) and hence this situation is a serious energy security concerns for many developed countries.

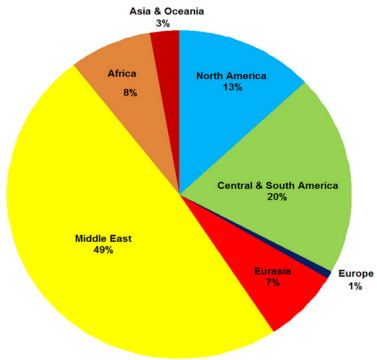

Figure 1.3: World oil reserves by region [11]

1.2 Natural Gas as an Alternative Fuel

One way to cope with the challenges detailed in the previous section is to shift to low-CO_2 alternatives to crude oil. Natural gas is one such fuel which has been most successful in replacing conventional liquid fuels like Diesel and Gasoline all over the world. Natural gas can be supplied from large fossil fuel reserves, from biomass and waste as bio-methane, where production comes from sustainable localized sources, and in the future also from "methanisation" of hydrogen generated from renewable electricity. All can be injected into the natural gas grid for supply from a single network. Natural gas offers a long-term perspective in terms of security of supply to transportation and a large potential to contribute to the diversification of transport fuels. It also offers significant environmental benefits, in particular when it is blended with bio-methane and provided that fugitive emissions are minimized. Published Well-to-wheel analysis data [12] on the total CO_2 emissions from a transportation system based on various alternative fuels shows that use of bio-gas produced from municipal waste and sewage can not only reduce CO_2 emissions, but may also contribute to negative emissions, that is, consume CO_2 from the environment.

The fact that Natural Gas can not only be *'found'* but also be locally produced from waste makes it a very attractive alternative fuel. There is however one major drawback of using natural gas, and that is emissions of methane (CH_4) into the atmosphere. With CO_2 assigned a Global Warming Potential(GWP) of 1, methane is estimated to have a GWP of 28-36 over 100 years, which means that even small amounts of methane released in to the atmosphere at any stage in the transportation system may offset the benefits of CO_2 emission reduction. But again, the *green* alternatives to fossil based natural gas as discussed earlier are still attractive due to the possibility of zero or even negative CO_2 emissions.

1.3 Research Motivation and Scope

Due to the reasons discussed above, natural gas engines are an attractive alternative to the present day diesel engine technology for heavy duty applications due also to reasons such as cheaper fuel, less expensive after treatment devices and increasing network of gas fueling stations worldwide. However, they lag behind in fuel efficiency and operating load range due to reasons like limitation in compression ratio, throttling losses, engine knock, high NO_x emissions and excessive exhaust gas temperature when operated with a stoichiometric mixture of fuel and air. This has led to an increasing use of the fuel-lean combustion strategies which yield lower in-cylinder temperature which reduces NO_x emissions and also heat losses, improving the thermodynamic efficiency. Fuel lean combustion also mitigates knock and hence enable high load operation. However, the lean limit is limited by the capability of the ignition system to reliably ignite the fuel-lean mixture. To overcome this limitation, alternative ignition strategies [13] like laser induced ignition [14, 15], diesel pilot injection [16, 17] and pre-chamber type ignition devices [18] have been proposed and evaluated by many researchers to a reasonable extent but only few have been successfully commercialized.

Application of laser induced ignition in combustion engines is still in the research phase and also difficult to implement in mobile applications due to complexity of laser ignition systems. Diesel pilot injection in natural gas engines has been implemented to some extent but mostly for stationary application due to fewer restrictions on space and ease of handling two fueling sub-systems. Recently, however, pilot ignited natural gas engines have been used for automotive applications [19]. As compared to these alternative methods, a pre-chamber ignition system offers a more simplified solution since it requires minimum or no engine modifications and is structurally less complex. It can also be considered more advantageous from the environmental perspective since it operates solely on natural gas, whereas a conventional fuel (diesel) still forms a significant part of the mix fed to a dual fuel engine. This is also evident from the current trend of major suppliers like Wärtsilä and MAN Diesel and Turbo gradually phasing out the dual-fuel gas engines and replacing them with pre-chamber ignited lean burn gas engines like the Wärtsilä 34SG and 50SG [20] and MAN 20V 35/44G [21].

Despite such benefits, to the best of the author's knowledge, pre-chamber ignition systems have not been implemented commercially in heavy duty gas engines for automotive applications. The reason is believed to be the inherent complexity of ignition resulting from such systems and that the performance is extremely sensitive to the control parameters. This partially explains its successful application in gas engines for power generation [20, 21] which are essentially constant speed and load type and hence more easily optimized.

Therefore, the motivation behind the research presented in this thesis was to study the application of the pre-chamber ignition system as an alternative ignition system in heavy duty natural gas engines used for mobile application, and to evaluate if the previously discussed benefits can be realized.

Research Motivation and Scope

The scope of this research was to study the influence of the pre-chamber ignition system on the performance and emissions characteristics of heavy duty natural gas engines under laboratory conditions. Various strategies of operating a pre-chamber ignition system were studied. Experiments were conducted to understand the requirements for geometrical and operating parameters of a pre-chamber ignition system to maximize fuel efficiency and reduce engine out NO_x emissions, since other emissions (HC and CO) are easily minimized using an oxidation catalyst.

Chapter 2

Background of Pre-chamber Ignition Systems

This chapter presents the history of the development of pre-chamber ignition systems, right from their conceptual origin up to the current state-of-the-art systems. Important milestones, discoveries and inventions are discussed in sufficient details to form a background for the studies presented in this thesis.

2.1 Origin and Early Concepts

The first four stroke engine where the air and fuel mixture was compressed prior to ignition was practically demonstrated by Nikolaus August Otto in 1867 [22]. Like the other concepts at the time, Otto's first engine used a flame to ignite the combustible mixture. Even though the use of jumping electrical spark for ignition had been demonstrated by Étienne Lenoir in his two stroke coal-gas powered engine in 1860 [22], it was not until the beginning of the 19th century that spark plugs along with the ignition magneto developed by Robert Bosch were used in a four stroke internal combustion engine.

Ever since, efforts have been made to overcome the inherent drawbacks of four stroke spark ignition engines, which can be summarized as:

- Limitation in compression ratio
- Throttling losses at part load operation
- Excessive heat loses due to high temperature combustion, and hence low fuel efficiency

Stratified charge engine concepts for four stroke spark ignition engines have been studied as a key remedy to these problems for over a century, and interestingly, N. A. Otto had discussed the stratified charge strategy already in 1867 [23].

He noted that to achieve better fuel efficiency, it is necessary that there is gradual development of heat and a corresponding gradual expansion of gases, instead of an explosion inside the combustion chamber. Otto, in his patent, wrote:

> *...no sudden explosion,...gradual development of heat and expansion, there will be no such losses of effect as result in gas engines of present construction through shocks produces by the sudden development of motive power, and by absorption of heat consequent upon the inability of the gases to expand with sufficient rapidity...*

In his patent, Otto proposes a strategy of charge stratification which is shown in Figure 2.1. As can be seen, several layers (a, b and c) of varying fuel strength are present with most of the fuel distributed close the ignition source (the flame in the lower right corner) and air near the piston. The benefits of such a distribution are controlled rate of combustion, and isolation of hot burnt gases from the combustion chamber wall during the expansion stroke to restrict wall heat transfer. He also proposes a method of regulating this stratification to control the power output from the engine.

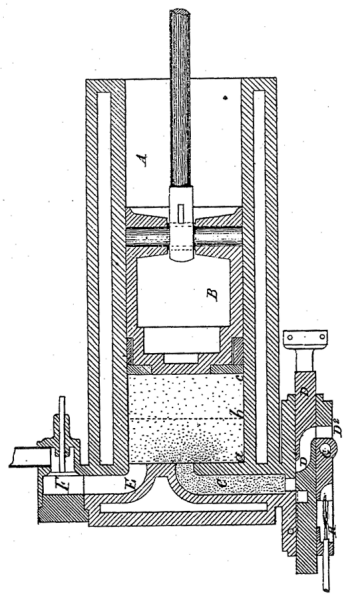

Figure 2.1: Proposed strategy of charge stratification inside the combustion chamber [23]

It was not until 1918 that Sir Harry Ralph Ricardo proposed the concept of containing these regions of varying fuel strengths in separate interconnected cham-

bers within the engine's combustion chamber [24]. He noted that with real working fluids, the specific heat (not the ratio) increases with an increase in temperature which results in less heating of working fluid by a unit fuel energy release. It is therefore of interest to keep the temperature during the cycle as low as possible which also reduces heat losses. An important motivation behind this invention was to enable *quantity governing* (diesel-like) in spark ignited engines and avoid the throttle and associated losses.

Figure 2.2 shows the layout of the first pre-chamber engine, the Ricardo *Three Valve Engine*. In this design, only air was inducted in the main combustion chamber (B) through the main intake valve (D), whereas a fuel and air mixture was inducted in the pre-chamber (G) through the *third valve* (H). The power output from the engine was governed by controlling the quantify of the fuel and air mixture inducted in the pre-chamber, while the mass of air inducted in the main chamber was unaffected, hence eradicating throttling losses.

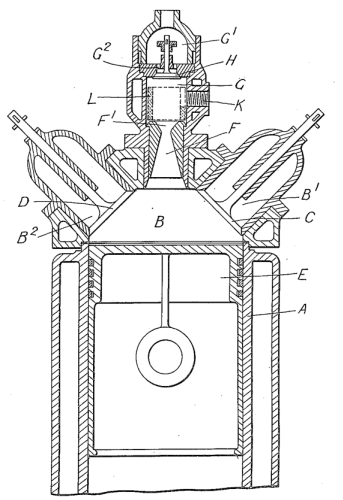

Figure 2.2: The layout of Riccardo's *Three Valve* Pre-chamber engine [24]

Following Ricardo's invention of the three valve engine, several other concepts along similar lines were proposed over the following decades. C. E. Summers [25] proposed an engine concept with a pre-chamber where the interconnecting channel was large enough for flames to be ejected into the main chamber. The pre-chamber was designed to assist this flame travel by inducing swirling motion. On the other hand, Marion Mallory [26] proposed the use of extremely small nozzle diameter such that there is sufficient pressure build-up inside the pre-chamber causing high velocity jets, which he claimed are more efficient in igniting a fuel-lean charge in the main chamber. Later, A. Bagnulo [27, 28] proposed a design with charge stratification even inside the pre-chamber to control the rate of energy release in

the pre-chamber. N. O. Broderson [29] proposed a design in which the pre-chamber volume was almost half of the engine's compression volume; and proposed different fueling strategies to control the power output from the engine. R. M. Heintz [30] proposed the use of a stand pipe, a pipe extending from the pre-chamber nozzle up to the spark plug electrode gap, in an attempt to reduce spark plug fouling due to deposits which was then common with pre-chamber engines. He also proposed use of tangentially drilled nozzle holes to induce a swirling motion inside the pre-chamber to improve mixing and reduce fuel-rich zones which contribute to deposits.

The developments in pre-chamber engines until around 1965 were, with some exceptions, based on the strategy of forming a close to stoichiometric mixture inside the pre-chamber at the time of spark while the main chamber was fuel-lean. The pre-chamber nozzle diameters were set such that the jets are of sufficiently high velocity promoting turbulent mixing in the main chamber. The ignition in the main chamber therefore relied on the high temperature of the stoichiometric combustion products from the pre-chamber and turbulent mixing in the main chamber.

2.2 The L.A.G. Ignition Process

A conceptually new way of operating a pre-chamber engine was developed in 1966, when a Russian scientist called Goossak Lev Abramovich (L. A. Gussak), proposed [31] the use of a very rich mixture (λ = 0.4-0.7) in the pre-chamber to produce a low temperature torch of incomplete combustion products (not a flame) containing chemically active species/atoms like CO, H_2, aldehyde and peroxide. This concept was called *'Lavinia Aktyvatsia Gorenia'* in Russian and hence is generally referred to as the LAG-Ignition process.

Gussak conducted several studies to understand the effect of fuel rich combustion in the pre-chamber on the main chamber combustion. He convincingly demonstrated the benefits of the fuel rich pre-chamber combustion strategy and while reproducing all of his important results here is not feasible, some of the key results are discussed in this section.

Figure 2.3 shows the effect of pre-chamber excess air ratio (denoted by α in this plot) on the flammability limit of the main combustion chamber for stationary flow experiments [32]. Another parameter used in the plot is δP, which is defined such that $\delta P = 0$ means that there is no pressure build-up in the pre-chamber, and $\delta P =$ 1 means infinite pressure build-up in the pre-chamber. Practically, δP is inversely proportional to the nozzle diameter, that is, a smaller nozzle diameter tends to increase δP. In Figure 2.3, there are two curves for a given value of δP, each corresponding to the extremities of the flammability limit in the main combustion chamber. One of the main observations from the plot is the apparent widening of the main chamber flammability limit as the mixture in the pre-chamber becomes fuel rich, specifically between α_{pc} of 0.5 and 0.8. Another important observation from this plot is that the flammability limit widens when δP increases from 0.2

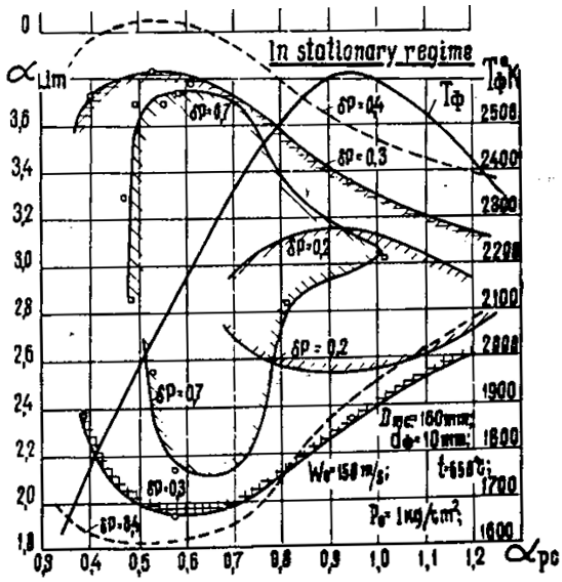

Figure 2.3: Effect of pre-chamber mixture strength of various operating parameters of a pre-chamber [32]

to 0.3, but then shrinks when δP is further increased to 0.7. This was a very important finding because most of the earlier pre-chamber concepts deliberately used small nozzle diameters to increase the jet velocity.

The combustion temperature inside the pre-chamber is also plotted in figure 2.3, which shows that the temperature peaks when the mixture inside the pre-chamber is slightly richer than stoichiometric, and reduces as the mixture becomes fuel rich. A practical implication of this finding is the reduction of NO_x formation inside the pre-chamber.

The reason behind the observed effect of nozzle diameter was explained by some fluid dynamic aspects of the interaction between the pre-chamber jets and the main chamber charge. Figure 2.4 shows the effect of δP on the resulting vortex formation in the main chamber. It can be seen, and expected, that the mixing vortices become smaller with an increase in δP, and Gussak argues that below a critical size, the vortices are unable to serve as sites for mixing and ignition in the main chamber. Hence a δP greater than a critical value reduces the flammability limit of the main chamber.

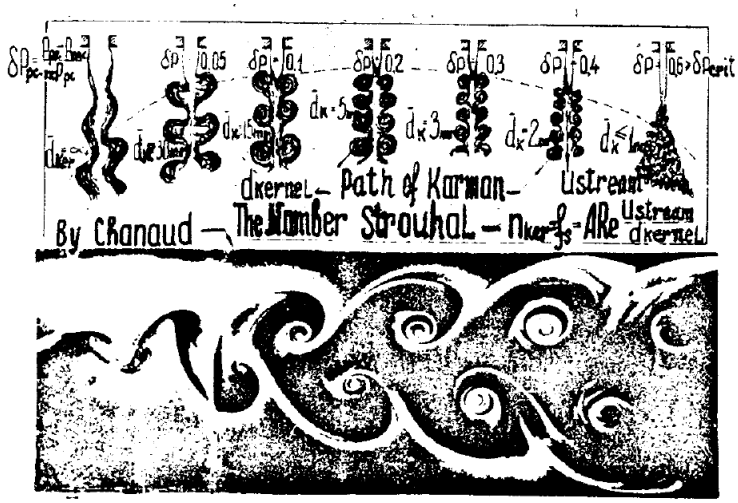

Figure 2.4: Vortex formation in the wake of pre-chamber combustion products flowing into the main chamber [32]

Further, fundamental studies on stationary flame combustion were conducted to understand the effect of pre-chamber mixture strength on the concentration of active species in the combustion products. Figure 2.5 shows the effect of initial fuel strength on the concentration of several intermediate combustion species seen in the flame. Each row corresponds to a particular set of active species like OH, CO, H_2 etc., and each column corresponds to a particular air-fuel mixture strength represented as excess air ratio (α). It can be seen that as compared to stoichiometric pre-chamber combustion (column 3), the concentration of all the active species increase as the fuel-air mixture becomes fuel rich, whereas all the active species are non-existent if the fuel-air mixture is made leaner than stoichiometric.

Another important aspect of pre-chamber ignition is the residence time of pre-chamber combustion products, which is defined as the time between their creation and their interaction with fuel-lean charge in the main chamber. The residence time is greatly controlled by the nozzle diameter, since a very small nozzle diameter imposes very high flow restriction between the chamber, elongating the residence time of pre-chamber combustion products. Gussak argues [33] that excessive residence time may cause the active species to recombine inside the pre-chamber, making the pre-chamber jets less reactive and hence reduce the main chamber flammability limit.

Figure 2.6 shows the experimental setup and results from a stationary flow study of the effect of the residence time (τ_r) of pre-chamber combustion products on the flame speed of the main flow. Referring to the experimental setup, it can be seen that the residence time was increased by introducing a elongation

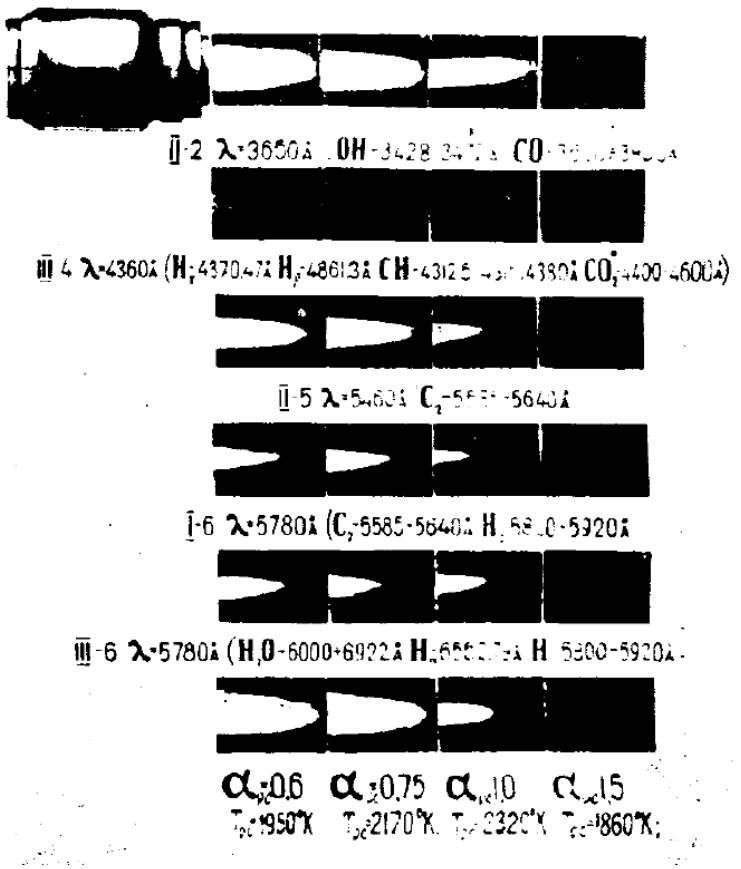

Figure 2.5: Streak photographs of stationary flame combustion - effect of fuel strength [32]

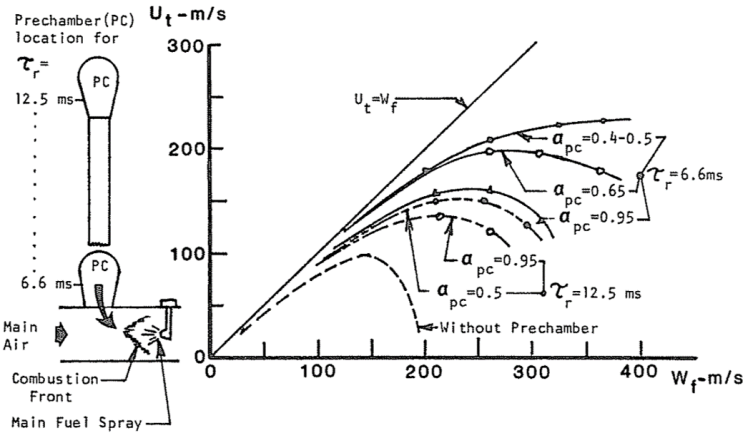

Figure 2.6: The experimental apparatus and the investigation results of the dependence of the turbulent combustion rate U_t on the stationary flow velocity W_f of the main mixture for different residence time of the pre-chamber combustion products and different pre-chamber mixture strengths [33]

pipe between the pre-chamber and the main flow. In the plot to the right, the turbulent combustion rate (U_t) is plotted against the stationary flow velocity (W_f) so that when the combuston rate equals the flow rate, the test point will fall on the line marked $U_t = W_f$. On the other hand, as the combustion rate lags behind the flow velocity, the test point lie in the area below that line. This plot is hence a measure of turbulent flow velocities achievable in the main flow for the given pre-chamber setting of mixture strength and residence time.

It can be seen from the plot that for ignition without a pre-chamber, a combustion rate of only 100 m/s is possible, after which the flame does not stabilize. For ignition with a pre-chamber, there are two other groups of curves in the plot, one for long residence time ($\tau_r = 12.5$ ms) and the other one for a short residence time ($\tau_r = 6.6$ ms). For each group, the pre-chamber mixture strength has been varied from close to stoichiometric to extremely fuel rich ($\alpha_{pc} = 0.4$). It can be seen that out of the two groups, the group with the shorter residence time is capable of stabilizing at much higher combustion rates of up to 200 m/s, whereas for the long residence time cases, the maximum combustion rate is restricted to around 150 m/s. Furthermore, for each residence time group, lower α_{pc} is capable of higher combustion rates in the main flow. This plot hence highlights the importance of residence time, and proves that fuel rich combustion in the pre-chamber alone does not guarantee improved ignition performance in the main chamber. The residence time, which is mainly affected by the nozzle diameter as discussed earlier, is also equally important.

2.3 Modern Systems

Alongside the development of the LAG-process of ignition, the pre-chamber ignition system found extensive commercial application in light duty engines, introduced primarily to reduce exhaust emissions with the fuel efficiency improvements being an additional advantage.

In the wake of the findings by Gussak on the importance of residence time, Newhall et. al. [34] developed a pre-chamber engine with the spark plug placed close to the interconnecting channel between the pre- and the main chamber. By this arrangement, the combustion products are directly discharged into the main chamber as the combustion proceeds towards the inner end of the pre-chamber. However, from the results presented, no significant benefits in terms of power output or fuel efficiency were found.

In 1975, Honda developed a combustion concept termed ***Compound Vortex Controlled Combustion (CVCC)*** using pre-chamber ignition with additional fueling. The particularity of the CVCC concept was three (or more) levels of stratification in the combustion chamber. The pre-chamber was deliberately over-fueled such that some of the fuel flows out of the pre-chamber. This over-flown fuel partially mixted with the main chamber charge during the compression stroke, but also formed a comparatively fuel-rich cloud of mixture around the pre-chamber nozzles. This formed three layers of stratification, first the pre-chamber being extremely fuel rich, then the fuel rich mixture cloud surrounding the pre-chamber and finally the fuel-lean charge further out in the main chamber. It was argued that this fuel-rich cloud provides a favorable environment for the pre-chamber jets to ignite the main chamber charge. The CVCC design demonstrated very low engine-out emissions and also high fuel efficiency.

Several other light duty pre-chamber engines were developed, like the Porsche SKS engine [35] and the Volkswagen PCI [36] with some particularities of their own but are not discussed further here.

Another major pre-chamber initiated combustion concept was developed by Oppenheim et. al. [37] during late 1980s under the name of ***Pulsed Jet Combustion (PJC)***. In his patent, he states that:

> ...shortcomings of similar devices of the prior art is that they are not capable of furnishing the required plumes **capable of entraining a sufficient amount of the compressed charge so that ignition and subsequent combustion occur in the interior of the eddies** of which the plumes are formed, but essentially ignite the main charge by establishing too readily the conventional flame fronts which traverse the charge at their own normal burning speed...

It is clear that in PJC, the pre-chamber was not just used as an ignition source for the main chamber charge, but the concept required formation of large mixing eddies or plumes within which the main chamber charge is consumed. Experiments

with the PJC system [38, 39, 40] showed that the dilution limit was only marginally extended from $\lambda = 1.66$ to 1.81. The fuel efficiency improved while the HC and CO emissions increased.

Considering very recent developments, in 2003, General Motors developed the Premixed Charge Forced Auto-ignition (PCFA) ignition concept that operated in a dual mode combustion system, with pre-chamber ignition at low load and conventional spark ignition at high load to avoid excessive pressure rise rates [41]. In 2005, Robert Bosch GmbH developed the Homogeneous Combustion Jet Ignition (HCJI) system [42] in which ignition inside the pre-chamber was achieved by auto-ignition by timely compression of pre-chamber charge by a separate piston. No published results of the performance of this system were found. In 2007, IAV GmbH and MULTITORCH GmbH developed pre-chamber spark plugs with pilot injection [43] demonstrating injection of hydrogen as pre-chamber fuel to further extend the dilution limit of the main chamber from $\lambda = 1.7$ to 2.

And finally, the most recent developments of commercial pre-chamber ignition systems have been done by Mahle Powertrain, under the name of Turbulent Jet Ignition – TJI [44]. Published studies with the TJI [45, 46] have shown extension of dilution limit excess air to around $\lambda = 2$. It was also demonstrated that the TJI system is capable of stable operation with extremely low ignition energies (10mJ) as compared to conventional spark ignition system which required a minimum energy of 40mJ at identical operating conditions.

The exact strategy of operation of these modern pre-chamber ignition systems is not explicitly published but most of them are reportedly operated with a stoichiometric or a slightly fuel rich ($0.9 < \lambda > 1$) mixture in the pre-chamber, and most of the published results are at low load operation in light duty engines.

It has been shown that pre-chamber ignition systems have undergone continuous development during the last century, but has not received as much attention as the other popular alternative to spark ignition, diesel pilot injection. This can partially be explained by the complex nature of the ignition resulting from a pre-chamber ignition system. To conclude this chapter, a quote from Sir Harry Ricardo's patent in 1918 [24] is reproduced below, which adequately summarizes the delicacy of pre-chamber ignition systems.

> *...if not just right, it may be very wrong; a very small change in form or dimension may upset the whole system...*
>
> *– Sir Harry R. Ricardo*

Chapter 3

Apparatus and Methodology

This chapter gives an overview of the experimental setups and diagnostic techniques used for studies presented in this thesis. The first half of the chapter briefly describes the experimental engines, the pre-chamber assemblies and associated instrumentation systems. The second half of the chapter presents the diagnostics techniques used to analyze experimental data and method of calculating several derived parameters which are used to understand the results.

3.1 Experimental Setups

The experimental setups were made up of an internal combustion engines in either multi- or single cylinder configuration and pre-chamber assembly suitable for the planned experiments. Both of these components were operated under flexible laboratory conditions which facilitated precise control of various operating parameters to an extent which is otherwise not possible on a production engine. Each experimental setup was controlled by a computer based control system and operation data was collected by a dedicated data acquisition system at varying rate. The sub-sections below discuss each of these sub-systems in further details.

Experimental Engines

Three different internal combustion engine setups were used during the course of research presented in this thesis. Each of these engines were characteristically different and hence were useful to study various aspects of pre-chamber ignition systems, however, this particular selection of engines was also influenced by their availability in the laboratory.

Volvo Multi-cylinder Engine

This engine was originally a 6 cylinder, 9.4 L diesel engine from Volvo Trucks which was modified to operate in spark ignition mode using natural gas as fuel under a reduced compression ratio of 12:1. The engine was equipped with a variable geometry turbocharger, a long route cooled EGR system, a multi-point gas injection system and an inductive type ignition system. Pistons with Quartette type combustion chamber design, which is known to generate high level of turbulence to enhance lean combustion [47], were used. This was the first and only engine setup that closely resembled a production engine and hence was used to perform relatively applied research studies with pre-chamber spark plugs. Further details about this engine can be found in Paper I.

Scania Single-cylinder Engine

This engine was a 6-cylinder heavy duty diesel engine from Scania which was modified to operate with one active cylinder of 2.12 L displacement volume. The remaining cylinders were motored without compression. The compression ratio of the active cylinder, which originally was 17.3:1, was reduced to 12:1 by introducing a spacer of appropriate thickness between the engine block and cylinder head. The original piston with a shallow bowl-in-piston design of combustion chamber was used. Natural gas fuel injectors were installed in the intake manifold for main chamber fueling and an inductive type ignition system with variable dwell time control was installed. A high pressure (10 bar-a) air reservoir fed the engine through a pressure regulator to adjust the intake pressure to the desired level. This single cylinder engine setup was prepared specifically for fundamental studies to understand the mechanism of pre-chamber ignition with auxiliary fueling. Special arrangements were made to accurately measure the air and gas flow to the engine though both the main and pre-chamber to calculate the excess air ratios in both chambers at the time of ignition. Further details can be found in Papers III & IV.

Wärtsilä Single-cylinder Engine

This engine was a large bore, medium speed, 6-cylinder Diesel-Natural Gas dual fuel engine from Wärtsilä which was modified to operate with one active cylinder of 8.8 L displacement volume, while the remaining cylinders were motored without compression. The geometrical compression ratio of the active cylinder was 13:1 but as the engine employed early intake valve closure strategy (Miller timing), the volumetric compression ratio was approximately 12:1. The original piston with an open combustion chamber design was used. Most of the other air supply arrangements were similar to those for the Scania engine but scaled up as necessary. One particular difference, however, was that the main gas admission valve on this engine required a pressure drop of less than 2 bar, and hence a pressure regulator was used in the main gas supply line. This pressure regulator was PID controlled for real time adjustments of the supply pressure depending on the intake

manifold pressure so that the quantity of gas injected for a set injection duration is unaffected. Most of the pre-chamber related arrangements were the same as for the Scania engine setup. Further details can be found in Paper VI.

Pre-chamber Assemblies

The pre-chamber assemblies, some bought from the market and others designed and manufactured in-house, were prepared to suit the engine and the experiments performed using them. Hence, three different pre-chamber assemblies were used in total out of which the first type used with the Volvo engine were bought from the market and were the simplest. They did not have any arrangements for additional fueling and were installed in place of the conventional spark plug hence requiring no modification to the engine. The pre-chamber assemblies used with the Scania and the Wärtsilä engines were custom made to suit the respective engine. They were also much more versatile and flexible with the parameters of interest in experiments.

Pre-chamber Spark Plugs

Pre-chamber spark plugs were used with the multi-cylinder Volvo engine for the studies presented in Papers I and II. They were produced by Multitorch GmbH in Germany and were bought off the shelf. A pre-chamber spark plug was essentially a conventional spark plug, with a hemispherical pre-chamber welded on its tip. An important difference, however, is that 4 pin-like arms extend out of the central electrode with their tips extending to the pre-chamber wall (ground electrode) forming a spark gap of approximately 0.3 mm. The pre-chamber volume was approximately 0.2 cm^3, which amounts to 0.141 % of the engine's clearance volume. Each pre-chamber had 5 nozzles of 1.1 mm diameter. For the set of experiments conducted with this pre-chamber and the Volvo engine, the pre-chamber volume and nozzle diameter settings were not specifically controlled since it was not required by the experiments. Pre-chamber spark plug nozzle orientation with respect to the combustion chamber cavity (Quartette design) was kept identical during all experiments. This pre-chamber spark plug was operated with the same spark ignition system used with conventional spark plugs during the experiments. Further details of the pre-chamber spark plugs can be found in Papers I and II.

Pre-chamber Assembly for the Scania Engine

As discussed earlier, the experiments conducted with the single cylinder Scania engine were relatively fundamental in nature and hence required a versatile and flexible pre-chamber assembly. Therefore, a pre-chamber assembly capable of fuel injection, spark ignition and pressure measurement was designed and manufactured. The assembly mainly comprised two parts, the pre-chamber head on which the required instrumentation was installed, and the pre-chamber body which could

be changed to change the pre-chamber volume. Two major experimental campaigns were conducted using the Scania engine and hence two versions of the Scania pre-chamber assembly were also prepared. They were essentially the same except for the use of a bigger spark plug (M10 instead of M8) and water cooled pressure sensor on the second version to overcome problems faced with the first version.

Fuel delivery into the pre-chamber was achieved using a miniature check valve, which was fed with natural gas at the desired injection time by a solenoid operated gas injector. Gas was supplied from high pressure (up to 200 bar) natural gas storage cylinders through a pressure regulator with manual control of downstream (pre-chamber injection) pressure of up to 25 bar-a. The mass flow rate of gas to the pre-chamber was measured using a thermal mass flow meter. Two surge tanks, of 2 liters each, were installed before the fuel injectors to isolate the pressure regulator and more importantly the flow meters from the pressure fluctuations caused by periodic injection of gas in the pre-chamber.

Apart from the gas injection valve, a spark plug and a pressure sensor was installed in the pre-chamber head. The relative positioning of these components was governed mainly by availability of space, but it was an intended design objective to place the spark plug closest to the center, and it was finally placed with a 2mm offset from the center axis. This was done to promote flame propagation in all directions so that most of the pre-chamber charge is consumed before the back-flow of charge from the main chamber occurs, and hence reduce unburnt hydrocarbon emissions due to incomplete combustion in the pre-chamber. This is one of the major design peculiarities as compared to other similar pre-chamber designs which can be found in literature [48].

For the first version of the pre-chamber assembly, which was used to study the fuel-rich pre-chamber combustion strategy (LAG process), the pre-chamber volume and nozzle diameter were set as close as possible to the recommendations by Gussak et. al [49] for the LAG process. Total number of nozzles were set to 8 for good spatial distribution of igniting jets ejected from the pre-chamber. This is also done to have a diesel-like initiation of combustion in the main chamber as the original diesel piston was used and the stock diesel injector for the Scania engine had 8 nozzles. The nozzles were drilled normal to the pre-chamber surface hence not contributing to formation of swirl due to in flow of charge during the compression stroke. The pre-chamber cone angle was set to 130° so that the nozzles are targeted to the same point of the piston bowl as by the diesel injector nozzles with a cone angle of 148° (geometrically).

Realizing the drawbacks of using an 8mm spark plug and an uncooled pressure sensor in the first version of the pre-chamber assembly, the second version was redesigned and built with a high performance M10 iridium tip spark plug and a water-cooled piezoelectric pressure transducer. This pre-chamber version was used for the experimental campaign to study effect of pre-chmaber volume and nozzle diameter in which 3 different pre-chamber volumes were tested. All these variations were achieved by changing the geometry of the internal cavity while

maintaining the same external dimension of the pre-chamber body, hence enabling the use of the same pre-chamber head and instrumentation set. Further details of each version of the Scania pre-chamber assembly can be found in Papers III and IV.

Pre-chamber Assembly for Wärtsilä Engine

The pre-chamber assembly designed for the Wärtsilä engine was conceptually similar to the one used in the Scania engine, except for the modifications required to suit the much larger cylinder head of the Wärtsilä engine. The assembly was completely redesigned externally to mimic the external dimensions of the engine's stock diesel injector. Further, due to the design of the cylinder head, the height of the pre-chamber body had to be increased but the ratio of the height of the pre-chamber body in the Scania and the Wärtsilä engine was the same as the ratio of cylinder bores of the engines. Another notable difference in this pre-chamber assembly was that the pre-chamber head was manufactured of Bronze while all other components in the assembly were made of stainless steel. This was done to overcome the thread-locking problem previously encountered in the Scania pre-chamber assembly since all components were made out of stainless steel. This assembly was used in an experimental study on scalability aspects of pre-chamber ignition and the dependency of performance of a pre-chamber of a given volume on the displacement volume of the engine. Thus, similar to the Scania pre-chamber assembly, three pre-chamber bodies with different internal volume were manufactured. Further details about the design of the Wärtsilä engine pre-chamber can be found in Paper VI.

Control and Data Acquisition System

Although three different engine setups were used, the architecture of their control and data acquisition system were essentially the same.

As illustrated in Figure 3.1, all control and data acquisition tasks were handled by a single computer which interacted with the test engine via three communication channels. The first channel was the high-speed data acquisition and control system card which was used for high speed (crank angle resolved) data acquisition from sensors for in-cylinder pressure, fast intake and exhaust manifold pressure etc., and also send signals to various controllers for gas injection, ignition, pressure regulators etc. For the multi-cylinder Volvo engine setup, the master PC was based on the GNU/Linux operating system and an in-house developed C++ based control and data acquisition system called 'DAPMEAS' was used. A Microstar 5400A (DAP 5400A) was used for all high speed DAQ and control purposes. For the Scania and the Wärtsilä engine setups, the control computer was Microsoft Windows based and a LabVIEW based control and data acquisition system was used. This LabVIEW based system comprised the main host computer and a target computer running LabVIEW real-time operating system with a PCIe-7842R

Multifunction RIO (Reconfigurable Input/Output) card.

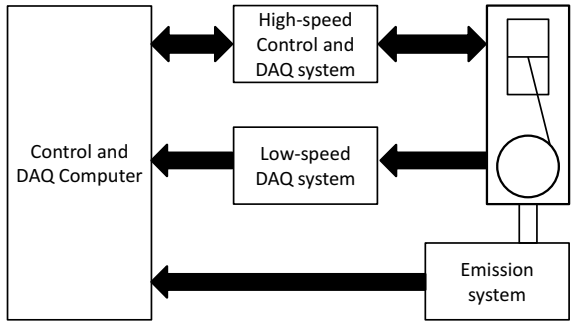

Figure 3.1: General layout of experimental setup.

The second communication channel was the low speed data acquisition system which operated at a data logging frequency of 1-3 Hz (depending on number of channels in use) and was used to record signals from various system level sensors for coolant temperature, lubricating oil temperature and pressure, intake air and gas flow rates, Lambda sensor etc. In all the engine setups, this function was accomplished using Agilent Technologies' 34970A Data Acquisition Unit capable of operating with 3 units of a 20 channel multiplexer card. This data acquisition unit communicated directly with the control computer (host computer) via a TCP/IP communication protocol and data was directly read by the main measurement and control program.

The third channel of communication was with the emission system which fed data on concentration of CO, CO_2, THC, NO_x and O_2 (Only in Engine setup 2) in the engine's exhaust. The measurement technique used for each of these species is detailed in table 3.1. The EGR rate was calculated by measuring the CO_2 in the intake and exhaust manifold. Data from the emission system was first fed to an intermediate server which then communicated with the main control computer via TCP/IP communication protocol.

Table 3.1: Measurement Techniques for different emission species

Species	Measurement Technique	Range
CO_2, CO	Non-Dispersive Infrared Detectors (NDIR)	0-15 %, 0-10000 ppm
THC	Flame Ionization Detector (FID)	0-4000 ppm
NO_x	Chemiluminescence Detector (CLD)	0-10000 ppm
O_2	Paramagnetic Detector (PMA)	0-25 %

3.2 Diagnostic Techniques

Several diagnostic techniques were used to analyze the data collected during experiments to understand the behavior of the in-cylinder combustion. This section begins by discussing the efficiency of various stages in which the fuel energy is converted into mechanical work in an internal combustion engine. The efficiency parameters which are extensively used during the studies presented in this thesis are then discussed in detail. The next diagnostic technique presented in the in-cylinder heat release analysis is based on the measured cylinder pressure. And finally, the method for estimating the excess air ratio inside the pre-chamber is briefly discussed.

Efficiency Parameters

An internal combustion engine is a heat engine which converts a fuel's chemical energy into mechanical work. In a reciprocating type engine operating on a 4-stroke cycle [50], like all engines used for studies presented in this thesis, this conversion happens in several stages which are depicted in a Sankey diagram in Figure 3.2. The text on the right hand side describes the flow of energy through each of these stages, presented as Mean Effective Pressure (MEP) which is defined as the work or energy per cycle normalized by the engine's displacement volume.

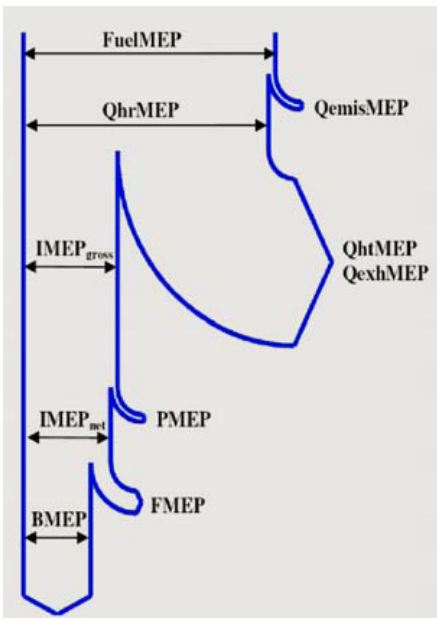

FuelMEP: Energy contained by the fuel
- QemisMEP: Chemical energy lost due to incomplete combustion
= QhrMEP: Chemical energy released in the combustion chamber
- QhtMEP/QexhMEP: Energy (heat) lost by heat transfer and exhaust
= $IMEP_{gross}$: Energy (mechanical work) transfered to the piston over compression and expansion strokes
- PMEP: Energy (mechanical work) lost in pumping work
= $IMEP_{net}$: Energy (mechanical work) transferred to the piston over the entire 4 stroke cycle
- FMEP: Energy (mechanical work) lost in overcoming mechanical friction
= BMEP: Energy (mechanical work) available at the output shaft

Figure 3.2: The Energy Cascade in an Internal Combustion Engine

As can be seen in the energy cascade, some amount of energy is lost in each stage and hence efficiency parameters are defined to evaluate each stage individually. The definition of selected efficiency parameters which are of importance to the following chapters are reproduced here.

Combustion Efficiency

The first stage is the combustion of fuel with an oxidizer during which the fuel's chemical energy (FuelMEP) is released in the form of heat in the combustion chamber (QhrMEP). The energy lost in this stage is expelled out of the combustion chamber as partially or completely unburnt fuel (QemisMEP), which can be estimated from the measured emission species like HC and CO in the engine exhaust. The efficiency of this stage is hence called Combustion Efficiency and is expressed by equation 3.1.

$$\eta_c = \left(\frac{QhrMEP}{FuelMEP}\right) = 1 - \left(\frac{QemisMEP}{FuelMEP}\right) \tag{3.1}$$

where, the various MEP values are calculated by normalizing the associated energy values by the engine displacement volume. As an example, equation 3.2 is an expression to calculate FuelMEP.

$$FuelMEP = \left(\frac{m_f \cdot Q_{LHV}}{V_D}\right) \tag{3.2}$$

where m_f is the mass of fuel per cycle, Q_{LHV} is the lower heating value of the fuel and V_D is the engine's displacement volume.

Thermodynamic Efficiency

The next stage is the conversion of heat released in the combustion chamber (QhrMEP) into mechanical work transfer to the piston during the expansion phase of the cycle. This stage usually contributes to the biggest energy loss in the entire process. As also shown in figure 3.2, energy loss during this stage is due to heat transfer (QhtMEP) and sensible heat of exhaust gases (QexhMEP).

The mechanical work transfer to the piston is calculated using the measured cylinder pressure and the cylinder volume calculated using the crank slider mechanism equations as discussed in [50]. The mechanical work transfer during the compression and expansion stroke is expressed as $IMEP_g$ and that transferred over all 4 strokes is expressed as $IMEP_n$, as shown in equations 3.3 and 3.4, respectively.

$$IMEP_g = \frac{\int_{-180}^{180} p \cdot dv}{V_D} \tag{3.3}$$

$$IMEP_n = \frac{\int_{-360}^{360} p \cdot dv}{V_D} \tag{3.4}$$

It can be noted that these definitions are based on fixed crank angle durations around the firing top dead center, and not on the valve timings of individual engines. Now, using these definitions, the thermodynamic efficiency is calculated by equation 3.5.

$$\eta_{th} = \left(\frac{IMEP_g}{QhrMEP}\right) = 1 - \left(\frac{QhtMEP + QexhMEP}{FuelMEP}\right) \tag{3.5}$$

Indicated Efficiency

The indicated efficiency is the efficiency of both the previously discussed stages combined. Two indicated efficiencies can be defined, gross and net, by calculating with the corresponding IMEP values. The gross indicated efficiency can therefore be expressed as equation 3.6.

$$\eta_{g,i} = \eta_c \cdot \eta_{th} = \left(\frac{IMEP_g}{FuelMEP}\right) \tag{3.6}$$

Combining equations 3.6 and 3.2, the gross indicated efficiency can be expressed as equation 3.7 which can be calculated using experimentally measured variables.

$$\eta_{g,i} = \left(\frac{IMEP_g}{\left(\frac{m_f \cdot Q_{LHV}}{V_D}\right)}\right) \tag{3.7}$$

The net indicated efficiency can be calculated in a similar way but will not be discussed here in detail as it has not been used in the presented studies.

Brake Efficiency

The brake efficiency is the efficiency of the entire energy cascade shown in figure 3.2, which accounts for all chemical, heat and friction losses in the engine. This parameter is therefore only calculated for the first experimental setup which was a multi-cylinder engine and whose mechanical power output was recorded. The brake efficiency is calculated by equation 3.8.

$$\eta_b = \left(\frac{BMEP}{FuelMEP}\right) \tag{3.8}$$

Heat Release Analysis

Heat release analysis is a diagnostic tool used to understand the rate and extent of the chemical energy release in the combustion chamber. Since this energy release generally happens during the closed part of the 4 stroke cycle (when valves are closed), the combustion chamber can be considered as a thermodynamically closed system, assuming that mass flow across system boundaries due to blow-by etc. is negligible. Given the instantaneous cylinder pressure and volume data, the first law of thermodynamics can be used to calculate the rate of energy addition to the system due to combustion. This calculation is presented at length in [50], and the final heat release equation can be expressed as equation 3.9

$$\frac{dQ_{net}}{d\theta} = \frac{\gamma}{\gamma - 1} \cdot p \cdot dV + \frac{1}{\gamma - 1} \cdot V \cdot dp \tag{3.9}$$

where Q is the energy released, γ is the instantaneous ratio of specific heat of the system of gases, p is the cylinder pressure and V is the cylinder volume. It should be noted that this equation yields the energy release excluding the energy lost due to heat transfer, and hence the heat release calculated using equation 3.9 is the net or apparent heat release.

To calculate gross heat release, the heat transfer was modeled as steady flow forced convection heat transfer to a solid surface and the heat flux is expressed by equation 3.10.

$$\frac{dQ_{ht}}{dt} = h_c(T_g - T_w) \tag{3.10}$$

where h_c is the heat transfer coefficient, T_g is the instantaneous cylinder gas temperature which is estimated using the ideal gas law, and T_w is the cylinder wall temperature. Several models exist for estimating the heat transfer coefficient and the model proposed by G. Woschni [51] was adopted for all calculations presented in this thesis. The heat transfer coefficient according to Woschni's model is given by equation 3.11.

$$h_c = 3.26 \cdot B^{-0.2} \cdot p^{0.8} \cdot T^{-0.55} \cdot w^{0.8} \tag{3.11}$$

where B is the cylinder bore, p is the instantaneous cylinder pressure expressed in kPa (unlike all other variables which are expressed in the SI system of units), T is cylinder temperature and w is the average cylinder gas velocity which is expressed by equation 3.12

$$w = \left[C_1 \cdot \bar{S}_p + C_2 \cdot \frac{V_D \cdot T_r}{p_r \cdot V_r} \cdot (p - p_m) \right] \tag{3.12}$$

where $\bar{S}_p$ is the mean piston speed, p_r, V_r, T_r are the working fluid pressure, volume and temperature respectively at some reference state (intake valve closure), and p_m is the motored cylinder pressure at the same crank angle as p.

The constants C_1 and C_2 used in equation 3.12 take different values during different periods of the cycle as given below.

Gas exchange period:	$C_1 = 6.18 + 0.417 \cdot \frac{v_s}{\bar{S}_p}$	$C_2 = 0$
Compression period:	$C_1 = 2.28 + 0.308 \cdot \frac{v_s}{\bar{S}_p}$	$C_2 = 0$
Combustion and expansion period:	$C_1 = 2.28 + 0.308 \cdot \frac{v_s}{\bar{S}_p}$	$C_2 = 3.28 \cdot 10^{-3}$

where v_s is the swirl velocity which is a function of ω_p, the rotation angular velocity of the paddle wheel used to measure the swirl velocity. Both of these variables are defined in equations 3.13 and 3.14.

$$v_s = \frac{B \cdot \omega_p}{2} \tag{3.13}$$

$$\omega_p = R_s \cdot (2 \cdot \pi \cdot N) \tag{3.14}$$

where R_s is the swirl ratio which was a known parameter for all the experimental engines.

Finally, combining equation 3.9 and equation 3.10 expressed in crank angle degrees, the gross heat release in the main combustion chamber can be expressed by equation 3.15

$$\frac{dQ}{d\theta} = \frac{\gamma}{\gamma - 1} \cdot p \cdot dV + \frac{1}{\gamma - 1} \cdot V \cdot dp + \frac{dQ_{ht}}{d\theta} \tag{3.15}$$

Model to Estimate Pre-chamber Excess Air Ratio

Tools like an oxygen sensor based Lambda sensing module and analysis of exhaust gases are generally used to estimate the overall air to fuel ratio in the combustion chamber of an engine, which, in an engine using pre-chamber, yields the overall air to fule ratio since it takes into account the total fuel injection in both the main and pre-chambers. For the studies presented here, it was necessary to estimate the excess air ratio of each chamber separately. The excess air ratio of the main chamber charge (λ_{MC}) was therefore calculated from measured air and fuel flow rates, however, direct measurement of pre-chamber excess air ratio (λ_{PC}) at the time of spark ignition is not straight forward as fuel-lean charge from the main chamber is continuously pushed into the pre-chamber during the compression stroke hence diluting the charge therein. Therefore, λ_{PC} is calculated from the measured fuel flow rate to the pre-chamber, and the previously calculated excess air ratio of the main chamber. The mass flow of charge into the pre-chamber during the compression stroke was calculated by equations for motion of slider crank mechanism. Gussak [49] used such a model but it was applicable for the case where a mixture of fuel and air is injected in both chambers, whereas in the experiments presented in this thesis, only fuel was injected in the pre-chamber. Hence a similar model was derived and can be found in Paper III.

Chapter 4

Experimental Studies

4.1 Un-fueled Pre-chamber studies

The first set of experiments were conducted using the multi-cylinder Volvo engine in which a pre-chamber ignition system without additional fueling (pre-chamber spark plugs) was studied and compared with conventional spark ignition system. The aim was to understand the main chamber ignition characteristics, dilution limit, maximum operating load and engine-out emissions with pre-chamber spark plug (PC.SP) as compared to with conventional spark plugs (C.SP), hereafter referred to as two cases. Four sets of experiments were conducted and selected results are presented here. Detailed results and discussion can be found in Paper I.

Heat Release Characteristics

The intention was to compare main chamber heat release characteristics for the two cases at the same operating points with respect to engine speed, load and spark timing, so as to compare flame development angle and combustion duration which are indicators of ignition and early flame propagation in the main chamber. Engine was operated at three speeds – 1200, 1500 and 1800 rpm, and three operating loads – 3, 6 and 9 bar IMEPg, with the spark timing held constant at 12 CAD bTDC for all the points. On this 9 point test matrix, dilution from stoichiometric operation (excess air ratio $\lambda = 1$) to the lean limit in steps of 0.1 was studied. This load range was selected to avoid the region of operation where the pre-chamber spark plugs cause charge pre-ignition, which is discussed in a later section.

Figure 4.1 is a plot of flame development angle which is defined as the time duration, in crank angle degrees, between the beginning of spark discharge and 10% accumulated heat release in the main chamber. It can be seen that ignition with pre-chamber spark plugs consistently results in shorter flame development angles than conventional spark plugs over the entire test matrix. Considering that

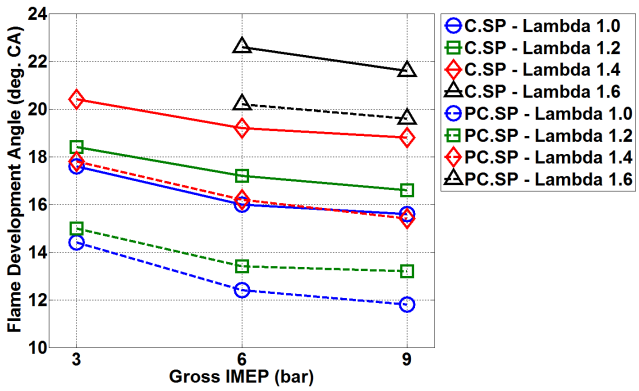

Figure 4.1: Flame development angle at 1500 rpm and under various load and dilution levels

the ignition from a pre-chamber spark plug is actually a two-step process, starting with ignition of charge inside the pre-chamber which results in formation of jets which then ignite the charge in the main chamber, it is interesting to note that these two steps are completed in less time than ignition with a conventional spark plug. This shows that multiple jets from a pre-chamber provide much higher ignition energy in the main chamber than a single point spark discharge. This effect, however, appears to diminish as the engine operates leaner as can be seen for the $\lambda = 1.6$ case. This can be attributed to over-leaning of the charge inside the pre-chamber in absence of additional fueling and a scavenging mechanism for the pre-chamber.

Figure 4.2 presents the comparison of combustion duration which is defined as the time duration, in crank angle degrees, between 10% and 90% accumulated heat release in the main chamber. Unlike flame development angle, the effects of ignition by a pre-chamber spark plug only become evident as the engine operates leaner. At stoichiometric conditions, both ignition systems result in similar combustion durations. It is expected that with the pre-chamber spark plug, multiple nozzles produce a spatially distributed ignition source resulting in onset of combustion at more than one locations simultaneously and hence the main chamber charge is consumed in a shorter time. But perhaps this effect is only significant when the engine operates lean with substantially reduced laminar flame speed of the main chamber charge.

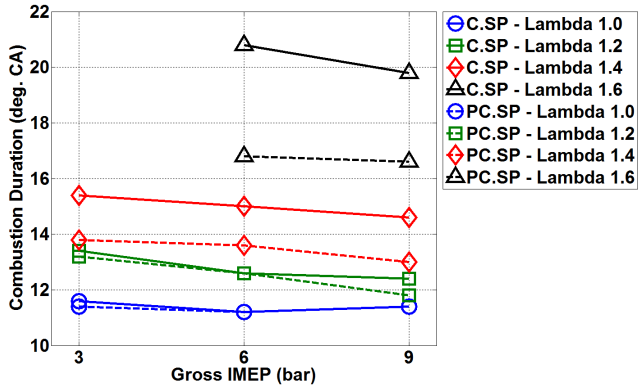

Figure 4.2: Combustion duration at 1500 rpm and under various load and dilution levels

Dilusion Limit

The maximum dilution with excess air and EGR while maintaining acceptable combustion stability were separately determined for each case. Experiments were performed at 1500 rpm engine speed and 5, 12 and 18 bar IMEPg engine load with knock limited maximum brake torque (MBT) spark timing for each operating point.

The dilution limit with excess air and EGR are shown in Figures 4.3 and 4.4, respectively. It can be seen that operation with pre-chamber spark plugs only marginally extend the dilution limit with excess air and EGR. This can again be attributed to over-leaning of the charge inside the pre-chamber due to the absence of a scavenging mechanism for the pre-chamber. At the beginning of every cycle, the pre-chamber is filled with residual gases and then fresh charge is pushed into the pre-chamber during the compression stroke. Hence at the time of spark ignition, the charge inside the pre-chamber is always more diluted than that in the main chamber. Hence at the lean limit, ignition inside the pre-chamber is itself a challenge.

Before proceeding further, it is important to mention that pre-chamber spark plugs caused charge pre-ignition at loads exceeding approximately 10 bar $IMEP_g$. It is believed that the pre-chamber surface becomes excessively hot and due to absence of an effective heat removal mechanism, the surface acts as a hot spot igniting the air-fuel mixture ahead of spark timing, which results in excessive cylinder pressure and unstable combustion. Due to this reason, it was not possible to operate the engine with stable combustion at loads exceeding 10-12 bar IMEPg without any dilution, and hence limited results are available in this regard in the following sections.

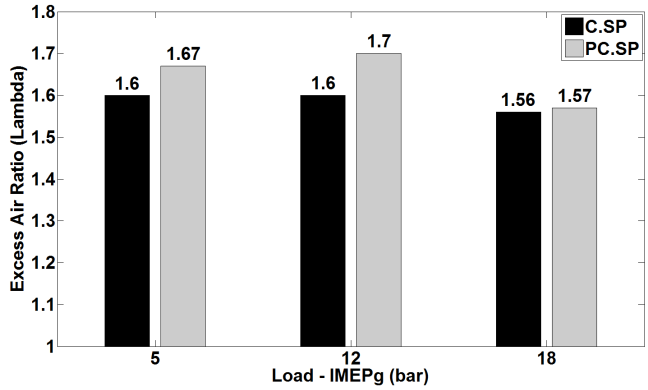

Figure 4.3: Comparison of dilution limit with excess air at 1500 rpm and various operating load

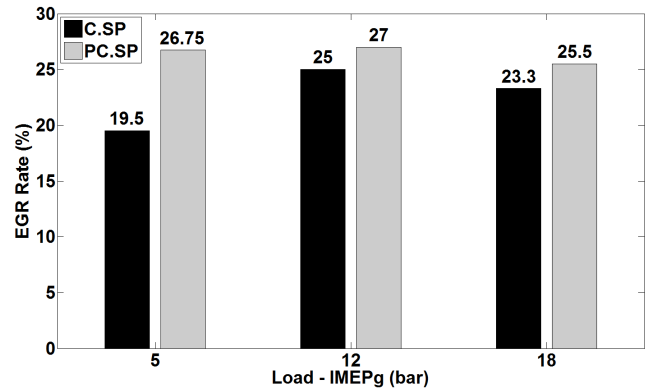

Figure 4.4: Comparison of dilution limit with EGR at 1500 rpm and various operating load

Minimum dilution required

Operating a natural gas engine at stoichiometric air to fuel ratio above certain operating load causes problems like excessive exhaust gas temperature which is unsuitable for the turbocharger and charge pre-ignition when operating with pre-chamber spark plugs. This means that a minimum amount of dilution, with either excess air or EGR, is always required when operating above a critical engine load, which was found to be in the range of 10 to 12 bar $IMEP_g$ for the experimental engine. This set of experiments served to determine this minimum dilution, while observing three main restrictions - exhaust temperature less than 700 °C, avoid charge pre-ignition and maintain combustion stability (COV of $IMEP_g$) below 5%.

Figure 4.5 shows the operating windows determined with each ignition system. As can be seen, the minimum dilution required increases with increasing load and this requirement increases very sharply with pre-chamber spark plug in order to avoid pre ignition. This factor also determines the maximum achievable operating load where the upper limit of dilution equals the minimum dilution required. It is interesting to note that the charge pre-ignition problem not only shrinks the operating window but also restricts the maximum load to 19 and 20 bar $IMEP_g$ with EGR and excess air dilution, respectively. On the other hand, it was possible to operate at loads up to 22.5 bar $IMEP_g$ under excess air dilution with a conventional spark plug as the limitation due to excessive exhaust gas temperature is comparatively less severe. It can hence be concluded that the benefits of slightly extended dilution limit with pre-chamber spark plugs are offset by the issue of charge pre-ignition, and hence the maximum operating load actually decreases with pre-chamber spark plug ignition.

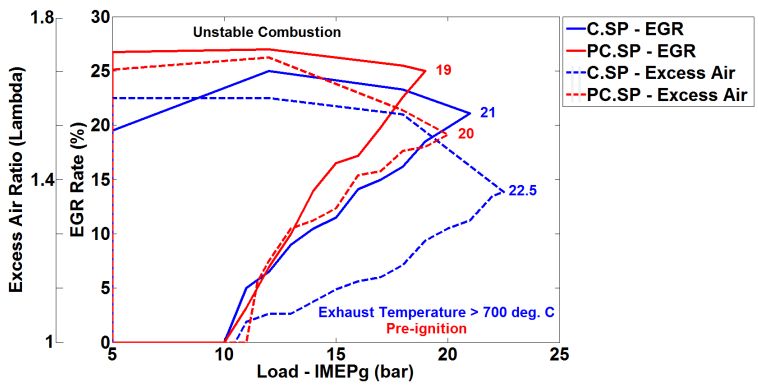

Figure 4.5: Comparison of minimum dilution required and available operating window at 1500 rpm

Combustion Stability

One of the benefits of pre-chamber ignition is the isolation of the spark plug from bulk charge motion in the main chamber and hence reduced cyclic variation of ignition and early flame development around the spark plug. A brief study of cycle to cycle and cylinder to cylinder variations was hence conducted to study the effect of pre-chamber spark plug on combustion stability. The cycle to cycle variation is the COV of $IMEP_g$ was calculated individually for each cylinder over a sample size of 200 cycles and then averaged, whereas the cylinder to cylinder variation is the COV of IMEPg between the 6 cylinders calculated individually for each cycle and then averaged over 200 cycles. As can be seen in Figure 4.6, both combustion variability parameters are lower for operation with pre-chamber spark plugs, with the difference being very significant near the dilution limit. This data proves that while the consistency of ignition with a conventional spark plug is highly affected by in cylinder flow characteristics and turbulence, ignition inside the pre-chamber and the following spatially distributed jets are less affected by in-cylinder flow characteristics.

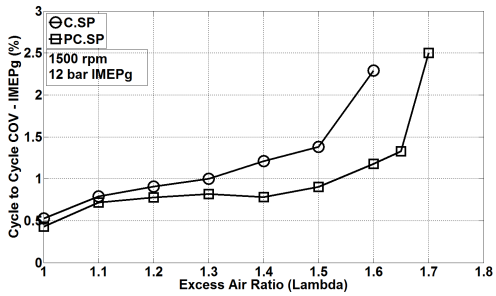

(a) Cycle to Cycle variations

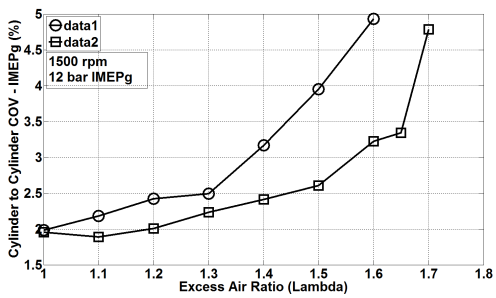

(b) Cylinder to Cylinder variations

Figure 4.6: Coefficient of variation in IMEPg at 1500 rpm, 12 bar IMEPg and dilution with excess air

Figure 4.7 shows the COV in IMEPg under EGR dilution conditions. Similar trends of better combustion stability with pre-chamber spark plug is visible also with EGR dilution, and are due to the reasons discussed above.

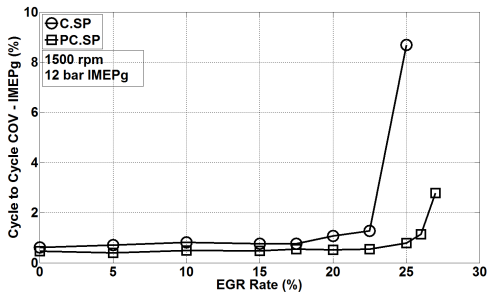

(a) Cycle to Cycle variations

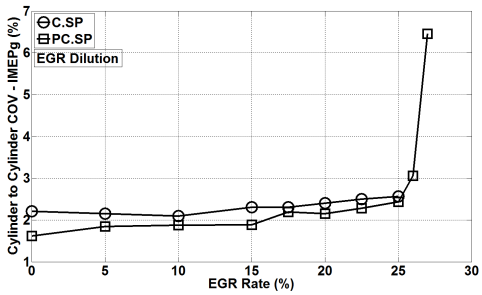

(b) Cylinder to Cylinder variations

Figure 4.7: Coefficient of variation in IMEPg at 1500 rpm, 12 bar IMEPg and dilution with EGR

From these results, it was clear that using a pre-chamber spark plug provides a more effective ignition source and also improves combustion stability, that is, the benefits of isolating the ignition source from main chamber charge motion and providing a spatially distributed ignition source were evident. However, in absence of additional fueling and hence over-leaning of charge inside the pre-chamber, there was only a marginal extension of the dilution limit with excess air and EGR. This restricts the use of pre-chamber ignition to achieve better efficiency and also restricts the maximum operating load. These results hence motivated the subsequent set of experiments to evaluate pre-chamber ignition with additional fueling.

Ion Currrent Sensing technique with Pre-chamber spark plugs

Ionization current sensing technique is well known for diagnosis of in-cylinder combustion and is widely utilized for closed-loop combustion control in spark ignition engines [52, 53, 54]. Therefore, a study was conducted to understand the response of the ion current sensing technique with pre-chamber spark plugs so that the applicability of such a proven technique with pre-chamber ignition systems can be assessed. This study is presented in Paper II and only the main conclusions are highlighted in this section.

It was found that with pre-chamber spark plugs, the amplitude of the first peak (chemical ionization peak) in higher but the second peak (thermal ionization peak) is very weak and even entirely missing at some operating points. Hence applicability of this technique to determine time of peak cylinder pressure (combustion phasing) is limited with pre-chamber spark plugs. Combustion stability parameters derived from the ion current signal do not correlate well with those derived from measured in-cylinder pressure. Hence the use of this technique to estimate combustion stability is also limited. It should however be noted that the response of the ion current technique is also affected by the design of the pre-chamber and relative positioning of spark plug electrodes, and hence the applicability of ion current sensing techniques with pre-chamber ignition systems cannot be completely ruled out based on these results.

4.2 Fueled Pre-chamber studies

Based on the results from the previous experiments, it seemed that additional fueling to the pre-chamber was necessary in order to overcome the over-leaning problem which restricts the dilution limit of the engine. Experiments were hence conducted with fueled pre-chamber ignition system. As discussed in Chapter 2, out of the two main strategies of fueled pre-chamber ignition system, the strategy of fuel-rich combustion in the pre-chamber was studied as it had documented benefits over the otherwise conventional strategy of operating with near stoichiometric mixture in the pre-chamber.

This study, as described in Paper III, was conducted to study the effect of additional fueling to the pre-chamber and more specifically, operating with a fuel-rich mixture in the pre-chamber. Experiments were performed using the Scania single cylinder engine setup and the first version of the pre-chamber assembly as discussed in section 3.1 and 3.1, respectively. The engine was operated with fuel-lean charge in the main chamber from λ_{mc} of 1.7 to the lean limit at a given λ_{pc}. This lower limit for λ_{mc} was chosen as it was the lean limit of operation with un-fueled pre-chamber spark plug previously discussed in section 4.1. λ_{pc} was varied from 0.7 to 0.2. There were two major reasons for selecting this range. Firstly, it was of interest to study combustion of fuel-rich mixture in the PC to operate with LAG-ignition process, and secondly, enriching the mixture in a small

size pre-chamber required injection of a very small quantity of fuel and the least quantity of fuel that could be injected in a controlled manner with the PC injectors resulted in a λ_{pc} of 0.7.

All experiments were performed with the intake manifold pressure of 1.5 bar-a which resulted in operating loads between 11 and 7.5 bar IMEPg. The spark timing was held constant for all test points at 17 CAD bTDC. This was done primarily to maintain similar flow field inside the pre-chamber at the time of ignition so as to facilitate a fair comparison between different test points, since it is known [55] that the flow field and turbulence inside the pre-chamber changes significantly towards the end of the compression stroke where the window of spark ignition time also normally lies. Gas was injected in the pre-chamber during the gas exchange period between 360 and 330 CAD bTDC to facilitate scavanging, and in the main chamber during the suction stroke starting at 330 CAD bTDC.

Dilution limit and NO_x emissions

The effect of reducing λ_{pc} on combustion stability, defined by COV of IMEPg, is presented for various main chamber dilution levels (λ_{mc}) in figure 4.8. It is clearly visible from the plot that upon reducing λ_{pc}, or in other words, operating fuel rich in the pre-chamber enables stable operation with leaner mixture in the main chamber. There is a distinct extension in lean limit for the case with $\lambda_{pc} = 0.2$ and there are two explanations for it. Firstly, since the concentration of active radicals formed is a non-linear function of degree of fuel-rich combustion, the combustion of a mixture of such high fuel strength may result in very high concentration of active radicals in the pre-chamber jets. Secondly, it could be related to over-flow of fuel from the pre-chamber which forms a cloud of fuel-rich charge around the pre-chamber assisting the ignition of pre-chamber jets and hence much leaner main chamber charge. Such three level charge stratification pre-chamber ignition system has been developed in the past, called Honda Compound Vortex Controlled Combustion (CVCC) engine [56].

The effect of extended dilution limit on indicated specific NO_x emission is plotted in figure 4.9. As expected, NO_x emissions reduce with increasing main chamber dilution. It can also be seen that for a given main chamber diluton, NO_x emission are higher as λ_{pc} reduces. This can be explained by the fact that as the fuel strength in the pre-chamber increases, ignition and early combustion phase in the main chamber is diesel-like mixing-controlled combustion with the mixing zones burning at high temperature close to stoichiometric conditions.

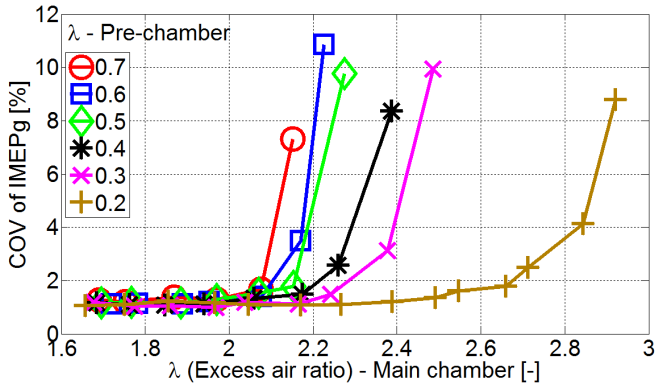

Figure 4.8: Effect of fuel rich mixture in pre-chamber on lean limit of operation

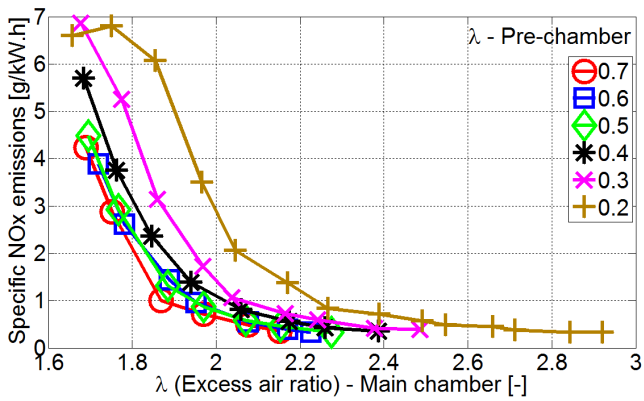

Figure 4.9: Effect of main chamber dilution at various λ_{pc} on indicated specific NOx emissions

Rate of initial heat release in the main chamber

A comparison of the rate of heat release in the main chamber, calculated by equation 3.15, for a main chamber dilution of $\lambda_{mc} = 2.0$ and various pre-chamber mixture strengths is shown in Figure 4.10. It can be seen that a very distinct first peak is visible in all the cases, which corresponds to the heat release due to combustion of partially combusted products carried by the pre-chamber jets to the main chamber. These burning jets serve as an ignition source for the remaining fuel-lean charge in the main chamber and hence the second and much higher peak of the heat release rate appears. The rate of heat release immediately following the first peak will represent the rapidity of onset of combustion in the main chamber. In order to quantify this parameter, the average rate of heat release in the main chamber starting immediately after the first peak (inflection point) until the crank angle of 10% accumulated heat released is calculated. This parameter is depicted in figure 4.10.

This initial rate of heat release is plotted in 4.11. Two major observations can be made. Firstly, for a given main chamber dilution, the rapidity of initial heat release increases by increasing the degree of fuel rich combustion in the pre-chamber. Secondly, this effect is amplified as the main chamber mixture tends to be more fuel-lean. This can be explained by the fact that partial combustion products from the pre-chamber react faster with a fuel lean charge due to greater availability of oxygen, hence causing rapid heat release by the combustion of jets and hence providing higher localized heating of the remaining charge.

A parameters more typical for conventional SI engines, the flame development angle, is also computed. In case of pre-chamber ignition, it is defined as the time duration between beginning of spark discharge inside the pre-chamber and 10% heat release in the main chamber. Figure 4.12 is a plot of flame development angle and it is evident that with increasing degree of fuel-rich combustion in the pre-chamber, the flame development angle reduces. It can also be noted that this effect increases with higher dilution in the main chamber. As expected, at a given pre-chamber mixture strength, the flame development angle is longer for higher main chamber dilution, but this difference diminishes as the pre-chamber mixture becomes more fuel-rich, and at λ_{pc} of 0.2, the flame development angle for all main chamber dilution is almost the same.

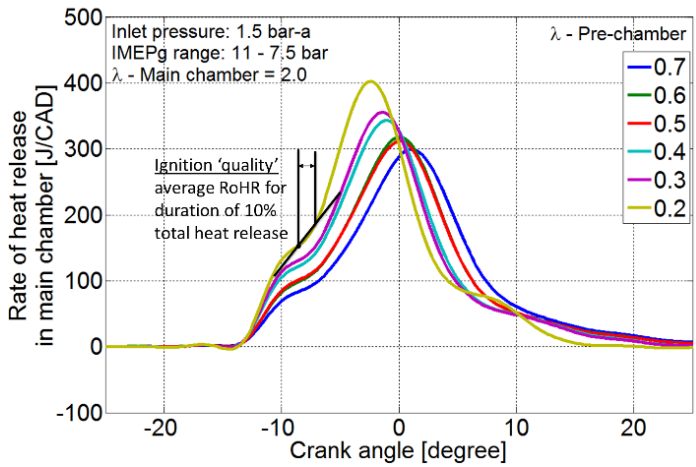

Figure 4.10: Comparison of heat release rates for λ_{mc} of 2.0 and various pre-chamber mixture strength

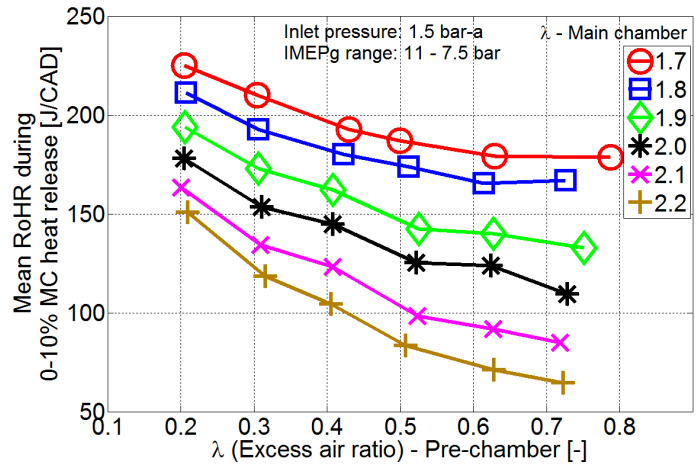

Figure 4.11: Effect of pre-chamber mixture strength on rate of initial heat release in main chamber

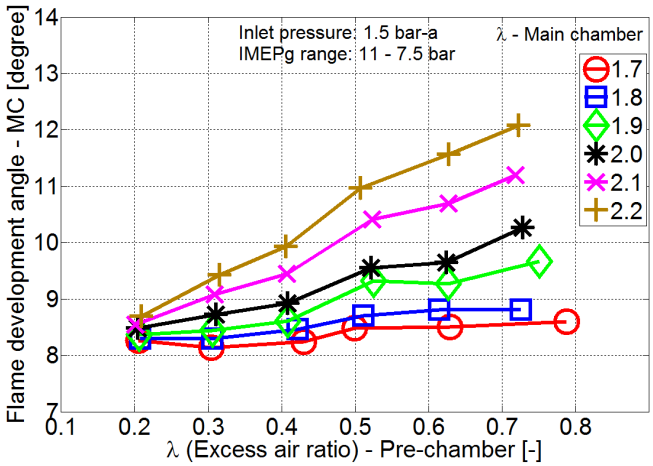

Figure 4.12: Effect of pre-chamber mixture strength on flame development angle

Efficiencies

Various efficiencies of the thermodynamic cycles are now presented. It should however be noted that all experiments were performed at a fixed ignition timing with an aim to study the ignition and early heat release. These operating points hence may not have the highest possible efficiency due to non-optimal combustion phasing.

The combustion efficiency (equation 3.1), as a function of pre-chamber mixture strength for various main chamber dilutions is plotted in figure 4.13. It can be seen that the combustion efficiency reduces with increase in main chamber dilution which is expected, but it is important to note that this fall in efficiency is greater when the pre-chamber is operated with the leanest mixture. In other words, for an example of $\lambda_{mc} = 2.2$ and $\lambda_{pc} = 0.7$ which has the lowest efficiency, by increasing the degree of fuel rich combustion in the pre-chamber, that is, by adding a very small quantity of additional fuel to the pre-chamber, it is possible to restore the combustion efficiency to close to that for other less fuel-lean main chamber conditions.

Figure 4.14 is a plot of gross indicated efficiency (3.6). This parameter is a product of combustion efficiency and thermodynamic efficiency and hence exhibits a non-linear behavior. It can be seen that the maximum indicated efficiency is at $\lambda_{mc} = 2.4$ and $\lambda_{pc} = 0.2$. This main chamber dilution seems to be a trade-off as between λ_{mc} of 1.7 up to 2.4, the gain in thermodynamic efficiency dominates over the loss in combustion efficiency, and visa-versa for λ_{mc} above 2.4.

From this campaign, it was clear that additional fueling in the pre-chamber, and forming a fuel rich mixture in the pre-chamber in particular, can considerably

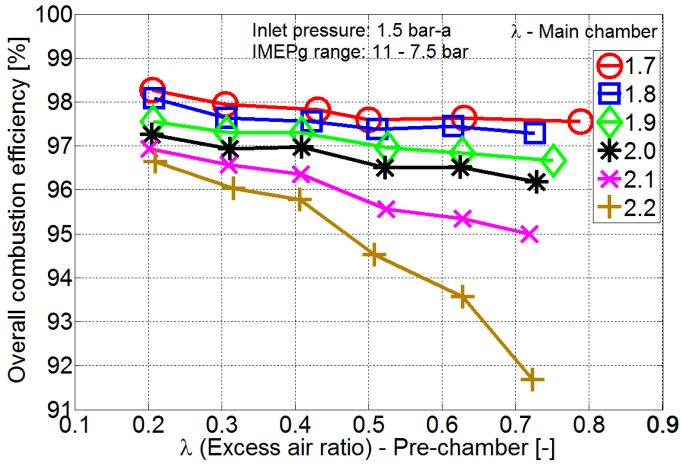

Figure 4.13: Effect of pre-chamber mixture strength on combustion efficiency

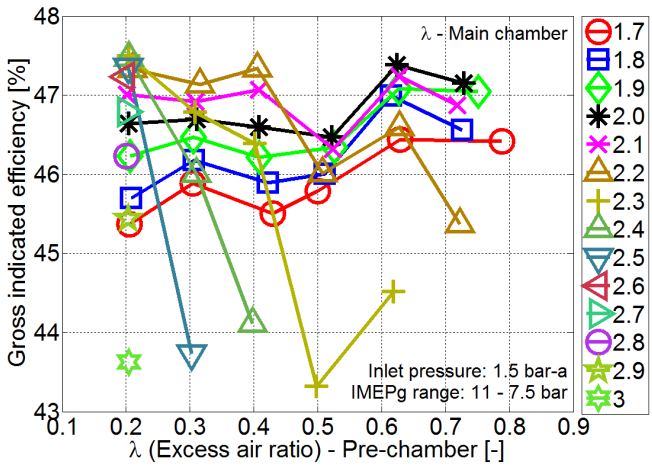

Figure 4.14: Effect of pre-chamber mixture strength at various λ_{mc} on gross indicated efficiency

extend the lean limit of the main combustion chamber which then leads to low engine out NO_x emissions and also improved indicated efficiency.

4.3 Effect of Pre-chamber Volume and Nozzle size

The effects of fuel rich combustion in the pre-chamber had been established, but in the previous experiments, the pre-chamber volume and nozzle diameter were set according to the recommendations for the LAG process [49]. However, these recommendation were derived from experiments conducted in either combustion vessels or a light duty engine setup with gasoline as fuel for both the pre- and the main chamber. Given that fuel rich combustion in the pre-chamber produces active radicals and their interaction with main chamber is governed greatly by the chemical kinetic properties of the fuel, it was necessary to determine the optimal setting of pre-chamber volume and nozzle diameter if natural gas is used as a fuel.

The aim of this study (Paper IV) was to investigate the effect of varying the pre-chamber volume and nozzle diameter settings around the recommended setting. Experiments were performed in two sets. The first set was focused on the study of the effect of varying pre-chamber volume and nozzle diameter on the resulting ignition and early heat release characteristics in the main chamber at similar operating conditions. Experiments were conducted at $\lambda_{mc} = 2$ and $\lambda_{pc} \approx 0.6$, which was deliberately chosen to avoid the pre-chamber fuel over flow regime which is expected to occur when λ_{pc} is below 0.4. The test matrix showing the pre-chamber volume and nozzle diameter settings is tabulated in table 4.1.

Table 4.1: Experimental matrix for the pre-chamber volume and nozzle diameter campaign

		A	B	C
		% Vc		
		1.4	2.4	3.7
		Pre-chamber volume [cm^3]		
		2.68	4.64	7.25
	Nozzle area ratio Apc/Vpc [cm^{-1}]	Nozzle diameter [mm]		
1	0.025	1	1.4	1.7
2	0.035	1.2	1.6	2
3	0.045	1.4	1.8	2.3

Note that the 3 different pre-chamber volumes are designated by classes A, B and C with A being the smallest and C being the largest pre-chamber. For each pre-chamber volume class, the nozzle area ratio (defined as the ratio of total area of connecting nozzles to the pre-chamber volume) was varied in 3 steps, designated as 1, 2 and 3 with 1 being the smallest and 3 being the largest nozzle area ratio.

The corresponding absolute dimension of nozzle diameter for each case is given in the table. Gussak's recommendations [49] for the LAG-process corresponds to case B2 and the variations around it are investigated in this study.

Apart from the steady spark timing tests, spark timing sweeps were also conducted to be able to compare combustion phasing dependent parameters like NO_x emissions. The second and relatively minor set of experiments conducted were to evaluate the lean limit of operation with excess air at various pre-chamber volume and nozzle diameter settings. Again, the spark timing was held constant at 17 CAD bTDC throughout this set.

Ignition and main chamber heat release

Data from the first set of experiments aimed at understanding differences in main chamber ignition behavior will be presented here. All the following figures represent data from 200 consecutive cycles for a particular operating point with the error bars representing 1 standard deviation. Figure 4.15 is a plot of variation in main chamber flame development angle. As discussed earlier, in a pre-chamber engine, this parameter is the total time needed for a sequence of events starting from initiation of combustion in the pre-chamber, flame development and propagation inside the pre-chamber, pressure rise due to heat release, development of pre-chamber jets and their mixing with main chamber charge and finally ignition and heat release in the main chamber charge. Hence this can be considered as a performance parameter of the pre-chamber as an ignition device instead of a conventional spark plug.

It can be seen from figure 4.15 that the flame development angle decreases with increase in pre-chamber volume. This is due to the difference in the quantity of combustible mixture in the pre-chamber. The duration of combustion and heat released in a smaller pre-chamber is comparatively less and hence pressure built up and the jets ejected are short lived. However, with increase in pre-chamber volume, higher heat release and hence higher pressure built up in the pre-chamber causes proper jet development which, upon interaction with main chamber charge, dissipates kinetic energy forming eddies which promote mixing. This theory is further supported by the observed effect of nozzle diameter ratio for a given pre-chamber volume in the same figure. The difference is clearly seen in smallest pre-chamber volume case which shows that the flame development angle is the shortest with the smallest nozzle diameter. This can again be attributed to the fact that for a given pre-chamber volume; a smaller nozzle diameter causes higher pressure build-up due to higher flow restriction and causes higher velocity jets. This high velocity imparts a more jet-like structure to the pre-chamber ejections resulting in better mixing and earlier inflammation of main chamber charge. However, this effect of nozzle diameter appears to be less significant as the pre-chamber volume increases which could be because the heat released and pressure build up in larger pre-chambers is sufficient for jet development and hence formation of initial mixing eddies is almost independent of nozzle diameter, or that the jets

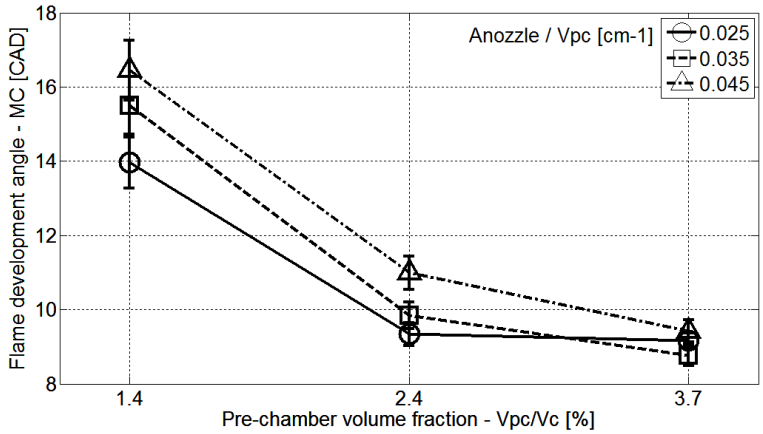

Figure 4.15: Effect of pre-chamber volume and nozzle diameter on main chamber flame development angle. Error bars represent 1 standard deviation

reach the combustion chamber wall in all cases and hence the mixing is not affected by nozzle diameter alone.

Main chamber combustion duration is plotted in figure 4.16. Overall they show the same trend of reducing combustion duration or faster combustion with larger pre-chamber volume. Jets from a larger pre-chamber engulf greater volume of main chamber charge and hence the portion of main chamber charge consumed by conventional flame propagation reduces. Another prominent effect visible in this plot is that of the nozzle diameter for all the pre-chamber volumes. Reduction in nozzle diameter causes higher pressure build-up and hence higher jet velocity, and at the same time, the mass flow rate through the nozzle reduces. It is therefore difficult to comment on the resulting effect on jet momentum but from the data, jet penetration (and hence jet momentum) seems to increase with reduction in nozzle diameter. Higher jet penetration causes charge ignition farther out in the main chamber hence reducing the time needed to consume the remaining main chamber charge.

To further evaluate main chamber ignition characteristics, the initial heat release in the main chamber (as defined in figure 4.10) is plotted for various test points. This parameter differs from flame development angle because this is related to pre-chamber jets and ignition of main chamber charge only and excludes the effect of all the preceding combustion events inside the pre-chamber. Hence this parameter is a direct comparison between jets from different pre-chambers. As expected, an increase in pre-chamber volume and reduction in nozzle diameter is seen to increase the initial heat release in the main chamber. The trend observed for pre-chamber volume can again be due to greater volume of charge engulfment by jets from larger pre-chamber and with smaller nozzle diameter, the higher velocity jets would promote turbulent mixing forming several small size eddies and

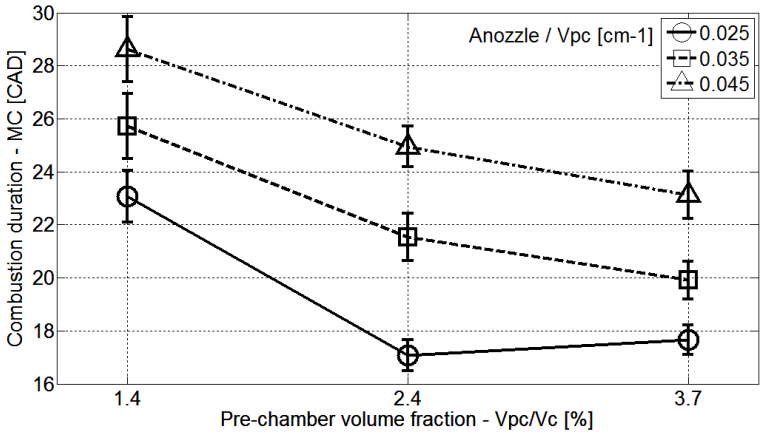

Figure 4.16: Effect of pre-chamber volume and nozzle diameter on main chamber combustion duration. Error bars represent 1 standard deviation

hence multiple sites of ignition. One thing to note however is that the change in pre-chamber volume from class B to C offers little benefit as compared to A to B.

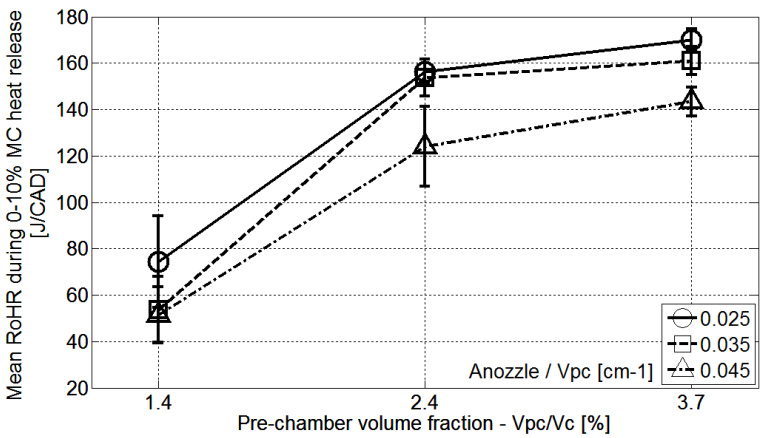

Figure 4.17: Effect of pre-chamber volume and nozzle diameter on initial heat release in main chamber. Error bars represent 1 standard deviation

Pre-chamber combustion

From the analysis so far, it seems that ignition and combustion inside the pre-chamber and resulting pressure built up across the nozzle significantly affects jet development and main chamber charge ignition. Therefore, the measured pre-

and main chamber pressures will now be analyzed. Ideally, to be able to comment on the nature of the energy release and thereafter the flow of energy from pre- to main chamber, heat release analysis of pre-chamber pressure data should be performed. However, this is not so straight-forward because pre-chamber alone is thermodynamically an open system and data on enthalpy flow to and from the pre-chamber is also required. It is difficult to estimate this parameter with sufficient accuracy due to limited knowledge of chemical and thermodynamic properties of species flowing at different times during the pre-chamber combustion event. An alternative to such absolute heat release analysis of the pre-chamber is discussed in [50] which essentially estimates the additional heat released in the pre-chamber using the measured pressure differential between pre- and main chamber, ΔP. Hence the measured P for the experiments performed are now analyzed as they are representative of the combustion, energy release and energy flow from pre- to main chamber in the form of jets.

Figure 4.18 shows sample traces of pre- and main chamber pressure after spark ignition for pre-chamber volume class A and different nozzle diameters. The effect of nozzle diameter on pressure built up is clearly evident and some parameters are defined to quantify the observed behavior. ΔP is the difference between the measured pre- and main chamber pressure as a function of time (or crank angle). x is defined as time duration between the instant when ΔP ($P_{PC} - P_{MC}$) exceeds the threshold of 0.5 bar and the time when the difference between a firing and motoring cycle main chamber pressure ($P_{MC} - P_{MOTORED}$) exceed a threshold of 0.5 bar which signifies ignition in the main chamber. This parameter basically represents the mixing time between pre-chamber jets and the main chamber charge before ignition. Parameter y is defined as the total time for which ΔP exists, with the thresholds being 0.5 bar at both the extremities.

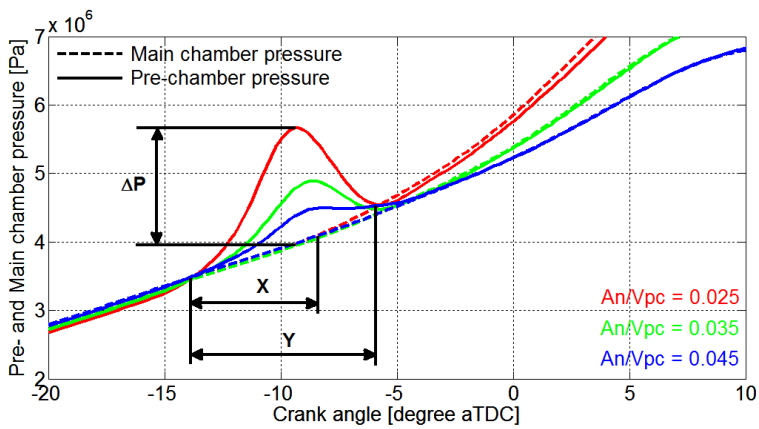

Figure 4.18: Example of Pre- and main chamber pressure after spark ignition at various nozzle area ratios

Effect of Pre-chamber Volume and Nozzle size

Figure 4.19 is a plot comparing the maximum ΔP for various cases. Referring to the effect of pre-chamber volume, ΔP is seen to increase from volume class A to B and this is due to higher heat release as a bigger volume of combustible mixture burns in a larger pre-chamber. However, this trend reverses while increasing pre-chamber volume from B to C which is counter-intuitive.

There are two explanations to this behavior with the first one being related to the effect of pre-chamber nozzle diameter on combustion inside the pre-chamber. As can be seen in table 4.1, at a given nozzle area ratio, the absolute diameter of the pre-chamber nozzle increases with an increase in the pre-chamber volume. The fluid dynamic effect of this change is a reduction in absolute flow restriction as the pre-chamber volume increases. This reduction in flow restriction increases the rate of enthalpy loss as ΔP starts developing hence restricting pressure and temperature built up inside the pre-chamber which ultimately slows down combustion in the pre-chamber. Hence the two factors which control the extent of combustion in the pre-chamber are firstly the absolute mass of combustible mixture in the pre-chamber, which increases with increase in pre-chamber volume; and secondly the flow restriction across the two chambers which reduces with increase in pre-chamber volume which, as discussed earlier, has a negative effect on combustion development. Hence it could be argued that upon increasing the volume from B to C, the effect of lower flow restriction has a dominant effect and hence reduces the extent of combustion in pre-chamber resulting in lower P.

The second explanation for reduced maximum ΔP is related to the timing of main chamber ignition. As seen in figure 4.15, the flame development angle is much shorter for the largest pre-chamber, and hence the pressure difference dies out earlier not because pre-chamber pressure drops but because the main chamber pressure start to rise following main ignition, hence reducing ΔP.

Regarding the effect of nozzle diameter at a given pre-chamber volume, the trend is as expected that smaller nozzle diameter causes higher pressure build-up across the nozzle due to higher flow restriction which promotes combustion in the pre-chamber.

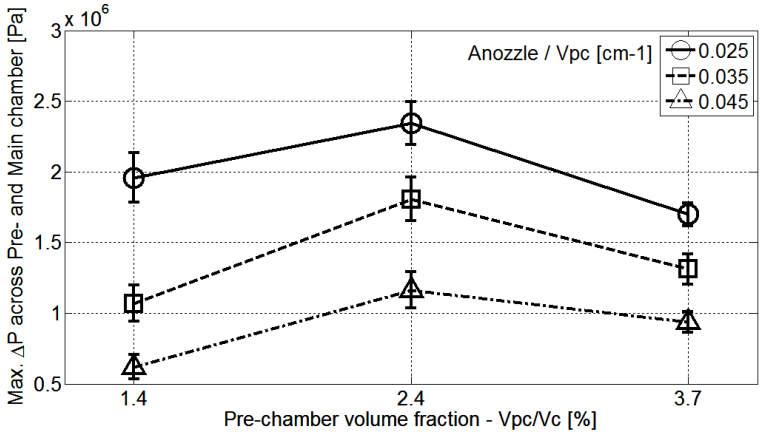

Figure 4.19: Maximum pressure difference across pre-chamber nozzle for various cases. Error bars represent 1 standard deviation

Lean limit and NOX emissions

Having discussed the fundamental characteristics of pre-chamber ignition; some parameters of practical interest are now discussed. One aim of an alternative ignition technique like pre-chamber ignition is to extend the lean limit of operation to improve efficiency and reduce NO_x emissions. If was found in previous studies that fuel rich combustion in the pre-chamber can considerably extend the lean limit with excess air. Figure 4.20 is a plot of lean limit with excess air while maintaining coefficient of variation (CoV) of $IMEP_g$ below 5%. It should be noted that the excess air ratio of charge fed to the main chamber is a control parameter and precise control over it is difficult at the lean limit. It can be seen from the plot that a larger pre-chamber volume enables stable combustion with a leaner charge in the main chamber. The explanation is similar to the one discussed for shorter combustion duration seen in figure 4.16. Jets from the larger pre-chamber engulf larger volume of main chamber charge reducing the volume of charge consumed by conventional flame propagation and hence reducing the cycle to cycle variation or misfire frequency.

It can also be seen that there was no resolvable difference in the lean limit due to different nozzle diameters for pre-chamber volume class A and B but for the volume class C, the lean limit is seen to increase as the nozzle diameter becomes bigger. This behavior is extremely counter-intuitive since for all other parameters studied, the smallest nozzle diameter seemed to result in better ignition. One explanation however relates to the basis of the LAG-ignition process [49], which is ejection of short lived active species by fuel rich combustion in the pre-chamber. The aspect of residence time as discussed by the original authors [49] states that if the flow restriction between the two chambers is too high, the pre-chamber

combustion product's residence time inside the pre-chamber increases and the active species recombine before they mix with the main chamber charge. Relating this to an earlier discussion in this article about the reason for lower maximum ΔP for volume class C, it can be argued that for the largest nozzle diameter, the degree of combustion in the pre-chamber is low and the mass flow of species is high which reduces the residence time of pre-chamber jets and hence the jets contain higher concentration of active species. Lower degree of combustion in the pre-chamber also means that a larger portion of pre-chamber fuel energy is released in the main chamber hence providing higher ignition energy.

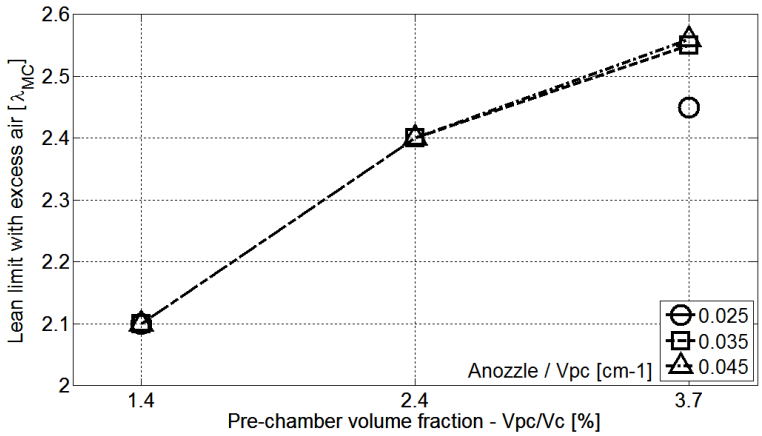

Figure 4.20: Lean limit of main chamber charge with excess air

Another parameter of practical interest is the concentration of regulated emission species in exhaust emissions. Unburnt Hydrocarbon (HC) and carbon monoxide (CO) are relatively easy to oxidize using after treatment devices. Methane oxidation is a known challenge [57] but this issue is not discussed further because HC emissions were not measured during the reported experiments. However, devices for NO_x after treatment when an engine operates with excess air are complicated and expensive. It is hence of interest to reduce in cylinder NO_x formation and therefore the effects of pre-chamber volume and nozzle diameter on engine out NO_x emission are now presented.

Figure 4.21 is a plot of indicated specific NO_x emissions at constant combustion phasing for various pre-chamber volume and nozzle diameters cases. As discussed earlier, spark timing sweeps were conducted and NO_x emission data for combustion phasing of 7 CAD aTDC is calculated by interpolation. Taking an average of all three nozzle diameter cases, it can be seen that NO_x emission increase with an increase in pre-chamber volume. This can be explained by an earlier discussion on the volume of main chamber charge engulfed by pre-chamber jets which combusts at near-stoichiometric conditions due to mixing with the jets. These high

temperature combustion zones are believed to contribute to NO_x formation. No clear trend of the effect of nozzle diameter is visible but it is interesting to note that the intermediate nozzle diameter, case 2, has lowest NO_x emissions of all the cases.

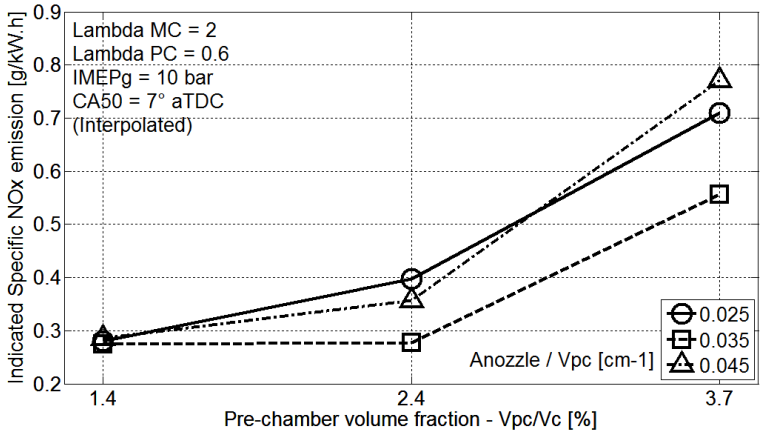

Figure 4.21: Indicated specific NOX emissions

In summary, also considering flame development angle data in Figure 4.15, it can be stated that increasing the pre-chamber volume fraction from 1.4% to 2.4% strongly reduces flame development angle but with minor increase in NO_x emissions, whereas further increase to 3.7% strongly increases NO_x emissions but with minor gain in flame development angle. Hence the volume fraction of 2.4% can be considered as an optimal trade-off between main chamber ignition characteristics and NO_x emissions. Regarding nozzle diameter settings, the smallest nozzle diameter area ratio of 0.025 cm^{-1} was found to reduce both the flame development angle and the combustion duration, but a larger nozzle diameter was found to extend the dilution limit of the engine. Hence, optimal setting for the nozzle diameter depends on case specific requirements of either faster combustion at a reduced dilution level, or an extended lean limit to reduce NO_x emissions.

4.4 Scalability Aspects of Pre-chamber Ignition

The aim of this study was to determine the dependency of the previously found optimal settings for the pre-chamber volume and nozzle diameter on the engine displacement volume. The research question was: *Is the performance of a pre-chamber, in terms of ignition and early heat release in the main chamber, dependent on the displacement volume of the engine?* Intuition suggests that combustion inside the pre-chamber and resulting ignition in the main chamber should be independent of engine size, since considering a pre-chamber as solely an ignition source

(like a spark plug), its performance should depend on its own volume and quantity of fuel at the time of spark, and not on the size of the main chamber. However, while operating with fuel rich combustion in the pre-chamber, it is known that partial combustion products are ejected into the main chamber and further oxidize as they mix with fuel-lean charge in the main chamber and hence the quantity of fuel-lean charge may have an effect on the early heat release in the main chamber. This study was hence conducted to understand the scaling requirements when applying pre-chamber ignition to engines of different displacement volumes. The study is presented here in brief and can be found in detail in Paper VI.

Experiments, similar to those conducted with the Scania Engine (section 4.3), were conducted on the Wärtsilä engine with a new set of pre-chambers, some of which were identical to the Scania pre-chambers in terms of absolute volume and others were identical in terms of relative volume. These relationships, along with the cross sectional views of the pre-chambers, are presented in table 4.2. As can be seen, the rows represent absolute pre-chamber volume in cubic centimeters and the columns represent pre-chamber volume relative to engine's clearance volume, expressed in percentage. Previous experiments conducted using a truck size engine from Scania and the corresponding pre-chambers used are also presented in their respective cells labeled Scania in the table, where the relative volume variation spanned from 1.4-3.7%. For the new set of pre-chambers for the Wärtsilä engine, four different pre-chamber volumes were studied as depicted in the cells labeled Wärtsilä in the table. The motivation behind this selection of volumes was to have two pre-chambers with the same absolute volume to those in Scania (row 2 and 3, bound by green border), and two pre-chambers with the same relative volume (column 3 and 4, bound by red border) to those in the Scania experiments.

Similar to the previous study, each pre-chamber had 8 nozzles. For the selection of nozzle diameters, the nozzle area ratio of 0.035 and 0.045 cm^{-1} was selected while the area ratio of 0.025 cm^{-1} was dropped since it resulted in very poor ignition in the main chamber and hence was of little interest. For these nozzle area ratios, the absolute nozzle diameter for each pre-chamber volume is tabulated in table 4.3. The numbering of each nozzle area ratio is also maintained the same as in the previous set of experiments (test matrix from the previous study in table 4.1) and hence row 1 (A1 to D1) is unused. Apart from these, pre-chamber volumes C and D were also operated with nozzle area ratio below 0.025, presented in row 0 in table 2. With this selection of nozzle diameters, the cases A2, B2, A3 and B3 resemble the Scania experimental cases such that both pre-chamber volume and nozzle diameter were identical. Cases C2, D2, C3 and D3 resemble the Scania experimental cases such that both parameters were scaled; and finally, cases C0 and D0 represent resemblance in terms of scaled pre-chamber volume but identical nozzle diameter. Further details about the experimental setup can be found in Paper VI.

Table 4.2: A matrix of comparison between the Scania and the Wärtsilä pre-chambers

V_{pc}/V_c [%] / V_{pc} [cm^3]	0.6	1	1.4	2.4	3.7
2.68			Scania 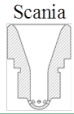		
4.6	Wärtsilä 			Scania 	
7.25		Wärtsilä 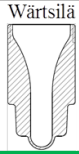			Scania 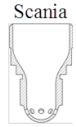
10.5			Wärtsilä 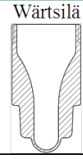		
18				Wärtsilä 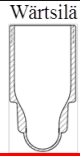	

Table 4.3: Test matrix for the Wärtsilä engine experiments

		A	B	C	D
		% V_c			
		0.6	1	1.4	2.4
		Pre-chamber volume [cm^3]			
		4.6	7.25	10.5	18
	Nozzle area ratio A_{pc}/V_{pc} [cm^{-1}]	Nozzle diameter [mm]			
0				1.2	1.6
1	0.025				
2	0.035	1.6	2.0	2.4	3.2
3	0.045	1.8	2.3	2.7	3.6

Before proceeding further it should be mentioned that the pre-chamber tip melted for case C0. This happened within a very short time (less than 10 firing cycles) and hence no data was recorded to study the pre-chamber behavior just before it melted. However, since for this case the nozzle area ratio is much lower than 0.025 cm-1, it is believed that excessive heat flux through the nozzles caused the metal in one of the inter-nozzle areas to melt and the pressure built up during the following cycle blew the pre-chamber tip off. It is already known from previous experiments (secton4.3) that for a given pre-chamber volume, reducing the nozzle diameter ratio from 0.045 to 0.025 cm-1 increases the magnitude of pressure differential between the pre- and main chamber and since the case C0 had an even smaller nozzle area ratio (0.0086 cm-1), the pressure build-up could have exceeded the mechanical strength of the pre-chamber. Following this melting event, the case D0 was excluded from the test matrix as it also had similar nozzle area ratio (0.0089 cm-1) as C0 and hence was prone to melting which may cause damage to the engine.

Ignition and Early Heat Release

The effect of pre-chamber volume and nozzle diameter was found to be similar to that in previous experiments with the Scania engine. The flame development angle and the combustion duration reduced with increase in the pre-chamber volume and reduction in nozzle diameter ratio. The initial heat release in the main chamber also showed similar trends. This set of results are therefore not reproduced here, and can be found in Paper VI.

Scaling Effects

This set of results presents a comparison of performance of the pre-chambers, which are similar on absolute and relative volume basis, in the truck size Scania engine and the large bore Wärtsilä engine. Comparisons are made both in absolute time

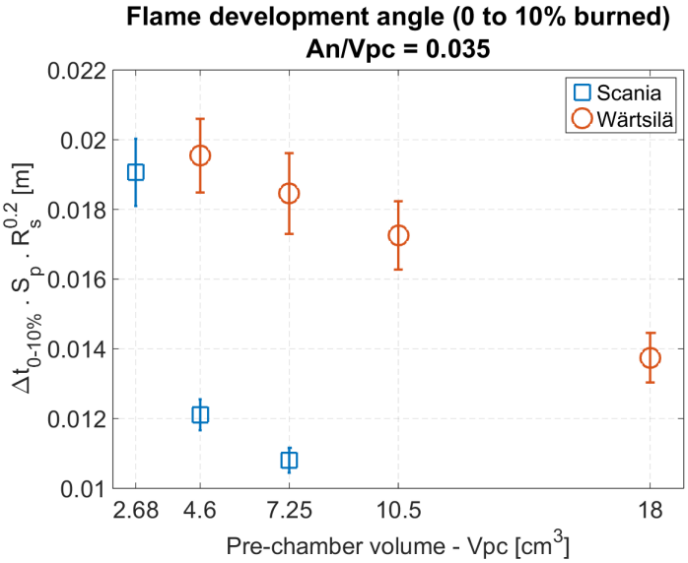

Figure 4.22: Normalized Flame development angle in absolute time scale plotted against absolute pre-chamber volume for nozzle area ratio of 0.035 cm^{-1}

and crank angle degree basis since the Scania engine was operated at 1200 rpm whereas the Wärtsilä engine was operated at 800 rpm. Considering a pre-chamber of a given volume solely a source of ignition used in two different engines, absolute time based comparison is interesting to understand the influence of fluid- and thermodynamic factors on ignition and following main chamber combustion. On the other hand, crank angle degree based comparisons are interesting because all engine control tasks like start of fuel injection and spark timing are controlled on a crank angle basis and hence such comparisons are of interest from an application point of view. Selected comparison on absolute time basis are reproduced in this section, with the others available in Paper VI.

Figure 4.22 is a plot of flame development angle in absolute time scale plotted against absolute volume of the pre-chambers used in both the engines. The flame development angle duration in absolute time is normalized based on the effect of mean piston speed, swirl and squish, as explained in detail in Paper VI. It is very clear from the plot that a pre-chamber of a given volume and nozzle diameter behaves very differently in a different engine. For the pre-chamber of 4.6 cm^3 volume, the flame development angle duration in Scania is half of that in the Wärtsilä engine. This proves that the ignition is greatly affected by the main chamber characteristics also, even though the processes inside the pre-chamber are less affected by the main chamber.

The same data as in Figure 4.22 is now replotted against relative pre-chamber

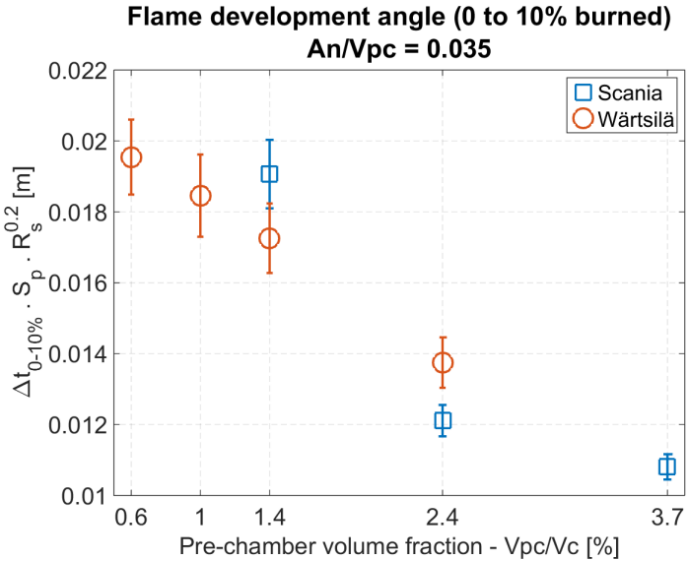

Figure 4.23: Normalized Flame development angle in absolute time scale plotted against relative pre-chamber volume for nozzle area ratio of 0.035 cm^{-1}

volume and is presented in Figure 4.23. A clear trend of reducing flame development angle with increase in relative pre-chamber volume is visible. Now, considering both figures 4.22 and 4.23, it can be stated that the jet energy required for main chamber ignition scales with the total mass of combustible mixture in the main chamber. A given pre-chamber with very short flame development angle in the Scania engine hence takes a much longer time to ignite the main chamber in the Wärtsilä engine. This highlights the importance of the mixing characteristics between the pre-chamber jets and the main chamber charge and also the initial heat release that occurs when the jets burn after mixing with fuel lean charge in the main chamber.

The total combustion duration data from both engines are now compared. Figure 4.24 is a plot of combustion duration in absolute time scale, normalized in the same way as the flame development angle, plotted against absolute pre-chamber volume. Again, the same trends of the combustion duration being very dependent on the total mass of combustible mixture is visible. There is an obvious reason that there is more mass to be consumed, but apart from that, for a given pre-chamber and its jet penetration distance, the ignition happens in the middle or the edge of the combustion chamber of the truck size engine whereas in a large bore engine with the same pre-chamber, the ignition occurs relatively close to the pre-chamber and hence it takes longer time to consume the charge further away from the point of ignition. Also, for a given pre-chamber volume, the ratio of the main

chamber volume engulfed by the pre-chamber jets to the combustion chamber volume reduces with an increase in the combustion chamber volume and hence the portion of main chamber charge consumed by conventional flame propagation increases.

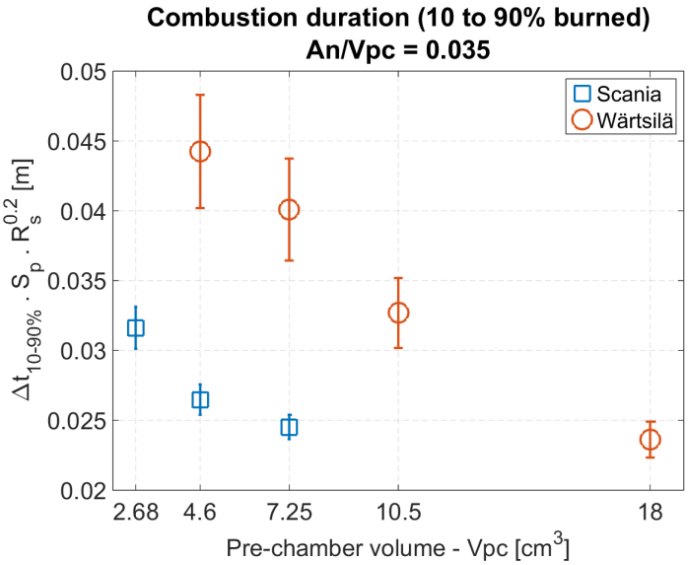

Figure 4.24: Normalized Combustion duration in absolute time scale plotted against absolute pre-chamber volume for nozzle area ratio of 0.035 cm^{-1}

The same data replotted against relative pre-chamber volume, as shown in Figure 4.25, shows a clear trend and also confirms the scaling effects previously discussed. It is interesting to note that unlike the flame development angle (Figure 4.23), the dependency of combustion duration on relative pre-chamber volume seems to be non-linear as the trends appear to flatten out beyond the relative volume of 2.4%. This can partially be explained by the previously discussed trends (section 4.3) of the flame development angle being relatively less affected by changing the pre-chamber volume from 2.4 to 3.7%, since the main combustion ignites before the combustion inside the pre-chamber ends. It can therefore be stated that pre-chambers with a relative volume greater than 2.4% do not reduce the flame development angle and combustion duration greatly but contribute to unburnt hydrocarbon emissions due to incomplete combustion inside the pre-chamber.

All other analysis is presented in Paper VI, but from the results it is clear that the performance of a pre-chamber of a given volume and nozzle diameter does depend, to a great extent, on the displacement volume of the main chamber.

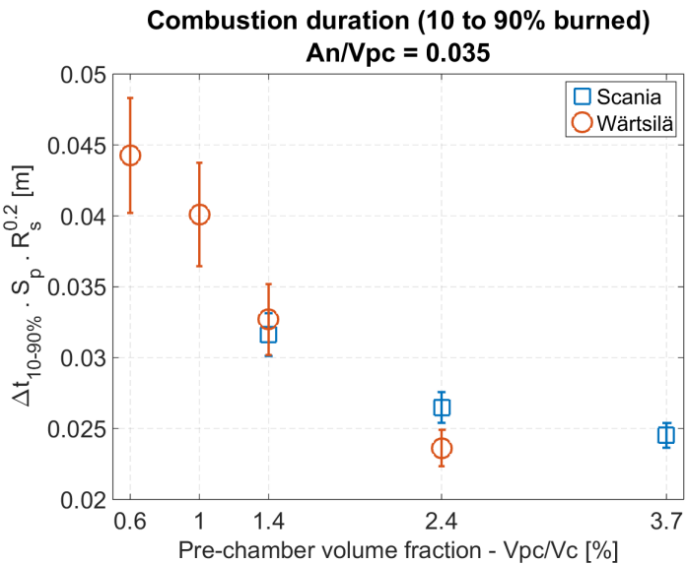

Figure 4.25: Normalized Combustion duration in absolute time scale plotted against relative pre-chamber volume for nozzle area ratio of 0.035 cm^{-1}

Chapter 5

CFD Simulations of Pre-chamber Jets' mixing characteristics

Experimental data suggests that increasing the volume of a pre-chamber provides better ignition, seen in terms of shorter flame development angle and combustion duration, but, with higher engine-out NO_x emissions. At a given pre-chamber volume, the smallest nozzle diameter (nozzle diameter ratio of 0.025 cm^{-1}) provides the best ignition performance. The observed trends of pre-chamber combustion and the resulting pressure build-up between the chambers were difficult to explain solely from the experimental data. It was therefore necessary to further scrutinize the data to understand the effect of the pre-chamber volume and nozzle diameter on the main chamber ignition.

The ignition from a pre-chamber system is a complex phenomenon governed by the chemical kinetic and fluid dynamic aspects of interaction between the pre-chamber jets and the main chamber charge. It is important to understand both these aspects to fully understand the behavior of a pre-chamber; but since detailed numerical simulations of combustion in an engine with pre-chamber was outside the scope of this reseach, relatively simpler CFD simulations were conducted to understand the fluid dynamic aspects alone. This investigation is carried out by performing 3D, transient, RANS type simulation on a 45° sector mesh of the combustion chamber with the experimentally measured pre- and main chamber pressure data as boundary conditions.

As discussed earlier with Figure 4.15, pre-chamber volume has a stronger effect on the flame development angle than the nozzle diameter. Whereas for combustion duration as seen in Figure 4.16, the nozzle diameter has a stronger effect than the pre-chamber volume. Following hypotheses were developed based on these results which are evaluated by CFD simulations:

- Jets from a larger pre-chamber have higher momentum which results in higher penetration speed and hence greater depth of penetration
- Higher momentum jets also generate turbulence early on in the main chamber which promotes mixing between the pre-chamber jets and the main chamber charge.
- For a given pre-chamber volume, a smaller nozzle diameter causes higher velocity jets which promotes mixing between the pre-chamber jets and the main chamber charge

5.1 CFD Simulation Setup

The CFD simulations presented in this article were performed using ANSYS® Fluent®, Release 15.0, and were of RANS type using the realizable k-ϵ turbulence model which can more accurately predicts the spreading rate of round jets [58], as are expected in the present case. A density based numerical solver with implicit formulation was used with second order upwind spatial discretization scheme for flow, turbulence and transient formulation. Species transport model, with a pre-existing mixture template of Methane-Air, was used to simulate the mixing between pre-chamber jets and main chamber charge. The time duration starting from spark discharge and equal to the flame development angle was simulated for each operating point in the Scania engine experimental matrix (table 4.1). Experimentally measured pre-chamber pressure was used as the boundary condition at the pre-chamber nozzle inlet. Further details of the computation grid, initial and boundary conditions can be found in Paper V.

5.2 Results and Discussions

This section presents the results obtained after simulation of all 9 cases. Data on properties of interest (species concentration etc.) were exported from the CFD software after every time step and were post processed using MATLAB where comparisons between all 9 cases were made. Selected results are discussed in this section. The legends (e.g. A3) in the plots correspond to a particular combination of pre-chamber volume and nozzle diameter as per table 4.1.

Depth of Penetration

Jet penetration behavior was determined by compiling data on methane concentration along the jet axis for each time setup for a given case. The resulting jet penetration behavior for all 9 cases is plotted in Figure 5.1.

It should be noted that the x-axis is the time after spark ignition in the pre-chamber, so the differences in the start of pre-chamber ejection are also included in the plot. As can be seen, the jet penetration curve flattens out after some time

which is either because the jet has reached the combustion chamber wall or has disintegrated before reaching the wall and does not travel any further. The end of the curve represents the end of the flame development angle in the respective case, i.e. the time of ignition and start of combustion in the main chamber.

It is apparent from the figure that there is a significant difference in start of ejection for case B, whereas the ejections for cases A and C start almost at the same time. This suggests that there are differences in the flow field inside the pre-chamber which affect the start of ejection. For case B, it can be seen that smaller nozzle diameter causes earlier ejection, which could be due to better mixing inside the pre-chamber during the flow of fresh charge from the main to the pre-chamber during the compression stroke. Whereas, the air-fuel mixture inside the pre-chamber in the largest nozzle diameter case is comparatively more stratified and hence combustion proceeds with a slower rate after spark ignition. Such differences are also expected in case A and C, but are perhaps not prominent at the current settings of volume and nozzle diameter for those cases.

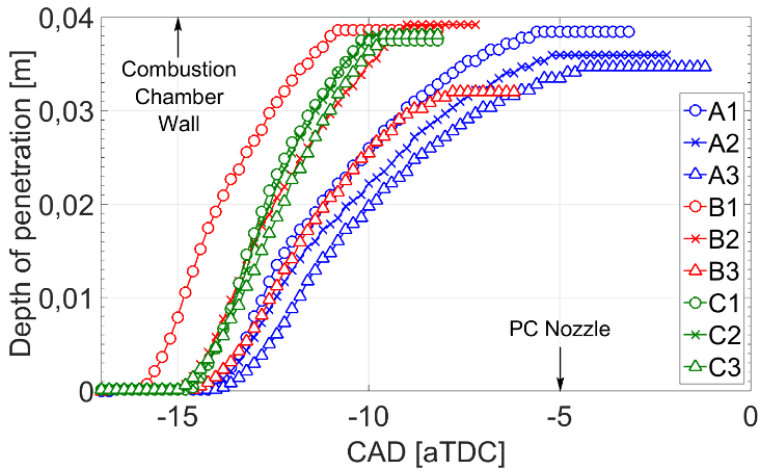

Figure 5.1: Depth of penetration of PC ejections for various volume and nozzle diameter cases.

It is also interesting to note the apparent change in the slope of jet penetration curves for the smallest volume case A. This suggests that for the time before the change in slope, jet head motion is governed by the momentum provided by the jet but further on, the jet loses its momentum and slows down as it penetrates further in the main chamber, which finally affects the depth of penetration.

In terms of depth of penetration, it can be seen that jets from the largest pre-chamber (C1 – C3) reach the combustion chamber wall for all the nozzle diameters, which is in line with the arguments of jet momentum presented earlier. For volume case B, jets for the smallest and intermediate nozzle diameter cases

reach the combustion chamber wall whereas the largest nozzle diameter case (B3) disintegrates half way. And finally for volume case A, only the jets for the smallest nozzle diameter case reach the combustion chamber wall. From these trends it can be deduced that nozzle diameter has a prominent effect on the depth of penetration and hence the distribution of active species in the main chamber. Jet penetration to the wall is beneficial because the recirculation zones created will enhance mixing in the main chamber, however, jet-wall interaction also increases heat transfer.

Figure 5.2 is a plot of average jet penetration velocity, calculated from the distance traveled by the jet during the time span between the start of ejection until the jet reaches the combustion chamber wall or stops traveling further. It can be seen that the rate of penetration is mainly affected by and is proportional to the pre-chamber volume. This is due to the differences in the absolute mass and hence the momentum of pre-chamber ejections, which increases with an increase in the pre-chamber volume. It should also be noted that since the nozzle diameter ratio is maintained constant, with an increase in pre-chamber volume, the absolute size of the nozzles increases and hence the jet core is thicker for a larger pre-chamber. It is hence capable of penetrating faster through the main chamber before the core breaks down. Regarding the effect of nozzle diameter, it can be seen that a jet from smaller nozzle diameter penetrates faster through the combustion chamber which is solely due to higher velocity and hence higher momentum for the jet.

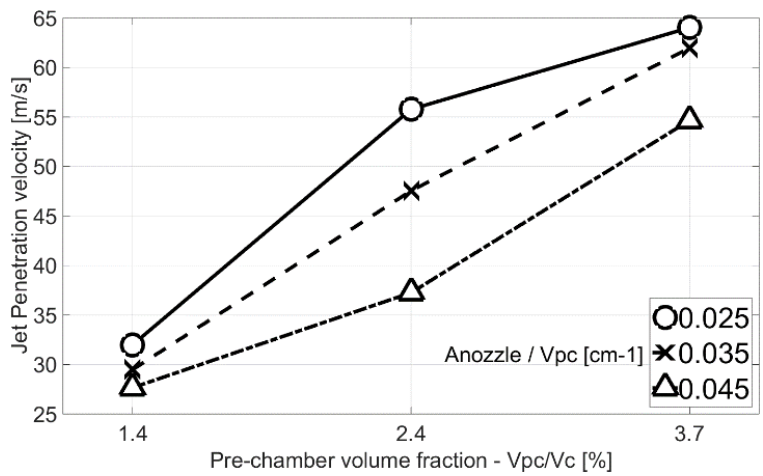

Figure 5.2: Depth of penetration of PC ejections for various volume and nozzle diameter cases.

Jet Development and Structure

It has previously (section 4.3) been hypothesized that in absence of sufficient pressure difference built-up between the chambers, or for a jet from small nozzle

diameter which is expected to have lower momentum; the pre-chamber ejections will not lead to jet development, but form a 'mushroom cloud' instead. To test this hypothesis, the relation between the instantaneous jet exit velocity at the nozzle (V_{Base}) and the instantaneous jet head velocity (V_{Head}) are compared. The hypothesis is tested by studying the differences in how well the jet head velocity follows the jet exit velocity, since in case of a mushroom cloud, the jet head velocity will drop faster and even to 0 in-spite of having a significantly high jet exit velocity. The jet exit velocity is obtained from the simulations by taking an average of velocity magnitudes for the nodes on the Jet Axis line which are within the nozzle length. The instantaneous jet head velocity is calculated by differentiating the curves in figure 5.1.

Figure 5.3 is a plot of the ratio of jet head velocity to jet exit velocity. Please note that unlike figure 5.1, the X-axis in this figure is time after the start of pre-chamber ejection, hence the curves are shifted in time to exclude the effect of difference in the start of ejection and to enable fair comparison between the jets alone. It can be seen from the figure that after almost 0.5 ms following start of ejections, the jet head velocity drops below 20% of the jet exit velocity in all the cases. This indicates that the differences in jet head velocity are not as distinct as expected and hence the structure of ejection is essentially the same without any indication of formation of distinct mushroom clouds in any cases. Never the less, the differences of interest are the rate at which this ratio falls from the beginning of ejection. The smallest nozzle diameter cases (A1, B1 and C1) are the first ones to slow down. The second set of curves are the intermediate nozzle diameter cases (A2, B2 and C2) and then the third set of curves for largest nozzle diameter cases (A3, B3 and C3) which slow down the latest. Even at a later time of 0.42 ms, it can be seen that the jet head velocity for the largest nozzle diameter cases is about 20-25% of jet exit velocity whereas for the smallest nozzle diameter case, the jet head velocity is below 10% of the jet exit velocity, suggesting a comparatively mushroom cloud like structure of ejection. Considering that these plots of jet head velocity are normalized over their respective nozzle exit velocity and hence are isolated from the effects of absolute mass ejected, it can be stated that nozzle diameter has a clear effect on the structure of the jet.

The structure of the jet will have a direct effect on the distribution of the pre-chamber jet contents in the main chamber. A jet like structure travels further in the combustion chamber and hence provides better spatial distribution of pre-chamber jet contents, whereas a mushroom cloud will deposit the pre-chamber contents closer to the pre-chamber and also limit the mixing between the ejected contents and main chamber given the lower jet head velocity. This, in effect, will prolong the combustion duration since a larger portion of the main chamber charge is consumed by conventional flame propagation. This is in conformity with the previous results obtained from engine experiments, as presented in Figure 4.16.

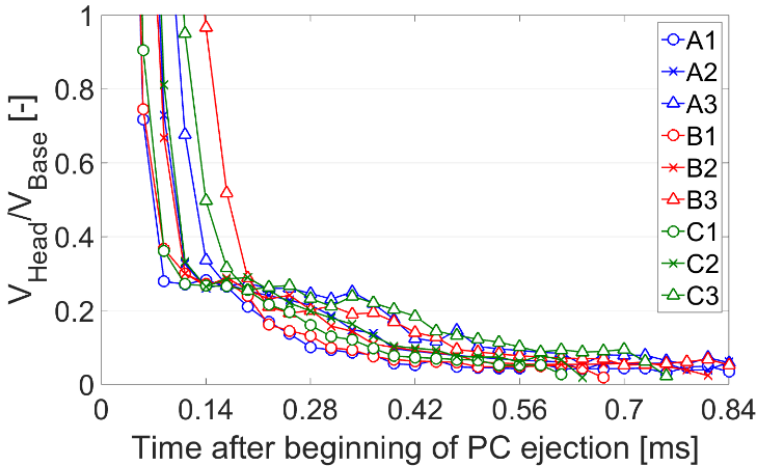

Figure 5.3: A ratio of jet head to the jet exit velocity for various volume and nozzle diameter cases.

Main Chamber Turbulence

Data on turbulence in the computational domain was also analyzed to understand the rate of production of turbulent kinetic energy in the main chamber due to the pre-chamber jets. It was found that for a given pre-chamber volume, a smaller nozzle diameter causes high velocity jets and hence higher turbulence generation in the main chamber, which will accelerate mixing in the main chamber. Also, it was found that the average turbulence level in the main chamber increases with an increase in the pre-chamber volume, which confirms the previously discussed hypothesis that jets from a larger pre-chamber engulf greater volume of main chamber charge. This effect can be related to the increase in engine out NO_x and shorter combustion duration. These results are presented in detail in Paper V.

The results of CFD simulations confirm some of the previously developed hypotheses, and also help explain the experimental results better. It should however be noted that these simulations only took into account the fluid dynamic aspects of the mixing characteristics in the main chamber while excluding the equally important chemical kinetic effects. An example of the implications is incorrect prediction of depth of penetration, since the head of the jet may react with the main chamber charge before the flame development angle duration has ended. This means that the predicted depth of penetration is longer than the actual depth of penetration and hence the jet penetration velocity and all other related data is erroneous. These results should therefore be used with caution.

Chapter 6

Summary and Conclusions

A series of studies were conducted to evaluate a pre-chamber ignition system as an alternative to a conventional open-chamber spark ignition system, as a means to improve fuel efficiency and reduce harmful emissions of internal combustion engines operating with gaseous fuels.

Both types of a pre-chamber ignition systems, with and without additional fueling to the pre-chamber, were studied. From the experiments comparing the performance of un-fueled pre-chamber spark plugs to that of conventional spark plugs on a multi-cylinder engine, it was found that using the pre-chamber spark plugs leads to a much shorter flame development angle and better combustion stability, but with minor extension in the engine's dilution limit which also restricts the improvement in fuel efficiency. Pre-chamber spark plugs were also found to cause pre-ignition beyond a threshold operating load, in effect reducing the maximum operating load of the engine. The reduction in emissions, specifically NO_x, was also minor.

Studies conducted with fueled pre-chamber ignition systems operating with a fuel-rich pre-chamber combustion strategy showed considerable extension of the dilution limit with excess air in the main chamber, with stable combustion at excess air ratios (λ) of up to 2.6. As a result, gross indicated efficiency of over 47% and engine out NO_x emissions below 1 g/kW.h were achieved. Following studies on the effect of the pre-chamber volume and nozzle diameter showed that increasing the relative pre-chamber volume up to 2.4% considerably improves main chamber ignition behavior without significantly increasing NO_x emission, whereas a further increase in the pre-chamber volume only contributes to higher NO_x emissions without any significant improvement in the main chamber ignition. The smallest nozzle diameter ratio of 0.025 cm^{-1} was found to provide best main chamber ignition but a larger nozzle diameter extends the dilution limit of main chamber combustion.

The dependency of these optimal settings on the engine's displacement volume, that is, the scaling requirements when applying pre-chamber ignition systems to

engines of various sizes were then studied by conducting experiments also on a large bore marine engine. It was found that the behavior of a pre-chamber of a given geometry and mixture strength is greatly affected by the properties of the main combustion chamber. The results showed that the pre-chamber volume needs to be scaled with the engine's displacement volume. Experiments on the large bore engine also demonstrated gross indicated efficiencies of over 50% at some operating points.

From these results, it can be established that a pre-chamber ignition system operating with a fuel rich pre-chamber combustion strategy is a very effective alternative to the conventional open chamber spark ignition system typically used in heavy duty engines running on gaseous fuels today. The pre-chamber ignition system has great potential in improving fuel efficiency and reducing engine-out NO_x emissions, hence addressing both global and local emission challenges.

Some key conclusions regarding the characteristics of pre-chamber ignition system that can be drawn from these studies are listed below.

- Isolating the spark gap from the main chamber charge motion by using a pre-chamber considerably reduces cycle to cycle variation in the ignition and main chamber combustion events.
- Un-fueled pre-chamber ignition systems, like a pre-chamber spark plug, are unable to extend the dilution limit of the engine due to over-leaning of the charge inside the pre-chamber.
- A pre-chamber ignition system without an effective heat removal mechanism may act as a hot spot in the main combustion chamber causing pre-ignition and hence unstable combustion.
- Additional fueling to the pre-chamber scavenges the pre-chamber at the beginning of every cycle and also forms a readily ignitable mixture in a very small volume around the spark gap, while the comparatively larger main chamber operates with an extremely fuel-lean charge. This configuration can results in very high indicated efficiency and reduce NO_x emissions.
- A relative pre-chamber volume of 2.4% is an optimal trade-off between main chamber ignition characteristics and engine out NO_x emissions.
- The nozzle diameter setting is case specific, depending on the relative importance of main chamber ignition characteristics and the dilution limit of the main chamber combustion.

Chapter 7

Suggestions for future activities

Even though the capabilities of pre-chamber ignition systems have been established and the optimal settings for the pre-chamber volume and nozzle diameter have been found, there is a need to further understand the fundamental mechanisms of the processes involved in pre-chamber ignition. There is a potential for further improvement and optimization and therefore, some research areas which the author believes should be further explored are listed below.

- **Mixture formation inside the Pre-chamber:** For the purpose of calculating the pre-chamber excess air ratio (λ_{pc}) in the studies presented in this thesis, the mixture inside the pre-chamber was assumed to be homogeneous. It is already known [59, 60] that the mixture inside the pre-chamber is stratified with most of the fuel in the top region of the pre-chamber and a fuel-lean main chamber charge at the bottom, with a mixing zone in between. Since fresh charge is continuously pushed into the pre-chamber during the compression stroke, it will be very difficult to achieve a homogeneous mixture of air and fuel inside the pre-chamber at the time of spark; but care should be taken to limit the charge stratification only along the axial direction. Radial charge stratification at any height inside the pre-chamber with isolated fuel-rich zone should be avoided. It is therefore very important to understand how the geometry of the pre-chamber and other operating parameters of the engine, like the engine speed and compression ratio, affect mixture formation inside the pre-chamber. CFD simulations are best suited for such studies, but even experimental studies with an in-pre-chamber sampling valve can be performed to understand pre-chamber mixture formation.

- **The relationship between the Pre-chamber Volume and Nozzle Diameter and the Combustion Inside the Pre-chamber:** The combustion inside the pre-chamber is one of the most important aspects which directly affects the contents of the pre-chamber jets. The main factors controlling pre-chamber combustion are the quantity of fuel, the volume of the pre-chamber, the surface to area ratio of the pre-chamber cavity and the nozzle diameter. Since the pre-chamber is thermodynamically an open system, there is a flow of mass from pre- to main chamber when combustion inside the pre-chamber starts. The fact that a measurable pressure difference exists between the chambers suggests that the rate of energy release inside the pre-chamber due to combustion is higher than the rate of energy loss due to mass flow out of the pre-chamber. Therefore for a given pre-chamber volume, the nozzle diameter plays the key role in controlling the extent of each of these processes and hence the contents of the pre-chamber jets. Insufficient nozzle diameter will impose very high flow restriction across the chambers resulting in high pressure and temperature buildup inside the pre-chamber. This in-turn promotes combustion inside the pre-chamber. On the other hand, excessive nozzle diameter will release the pressure very rapidly and hence the combustion inside the pre-chamber may quench, resulting in un-burnt fuel in the pre-chamber jets. And as can already be appreciated, this behavior is greatly affected by the chemical kinetic properties of the fuel being used and hence studies conducted with a particular fuel are difficult to generalize. This phenomenon should therefore be studied by modeling the combustion inside the pre-chamber for various pre-chamber volume and nozzle diameter cases. Figures like 7.1 and 7.2 can be expected out of the proposed modeling activity. Figure 7.1 shows the flow of various species for the duration of positive ΔP between the chambers. Due to the axial charge stratification, the contents that first flow out of the pre-chamber is the main chamber mixture (MC mixture) and as time progresses, the flow of partial combustion products (Formaldehyde and CO) starts to emerge out of the pre-chamber. This process will be affected by the geometry of the pre-chamber and the surface to area ratio which governs heat transfer.

  A similar modeling study of the effect of nozzle diameter for a given pre-chamber volume may result in figure 7.2 which shows the total mass of a given species that flows out of the pre-chamber during one ignition event. The plot suggests that with insufficient nozzle diameter, the combustion inside the pre-chamber is relatively complete and hence the total mass of partial combustion products is high, but for a larger nozzle diameter, the combustion inside the pre-chamber stalls and hence the mass of partial combustion products reduces while the mass of main chamber charge being pushed back into the main chamber as the pressure rises, increases.

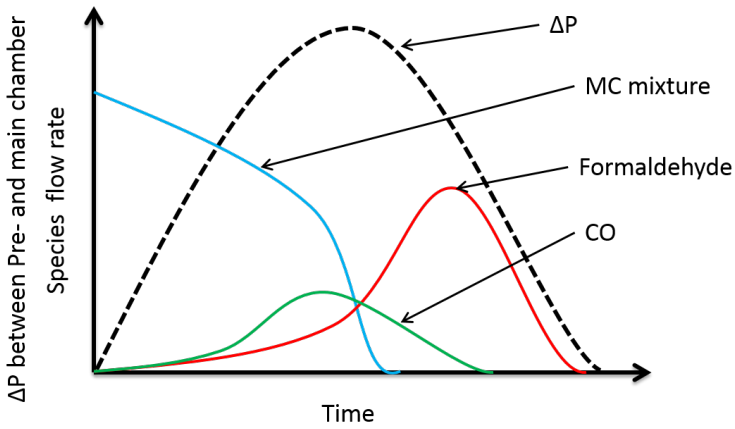

Figure 7.1: Hypothesized model output for species flow rate from the pre-chamber

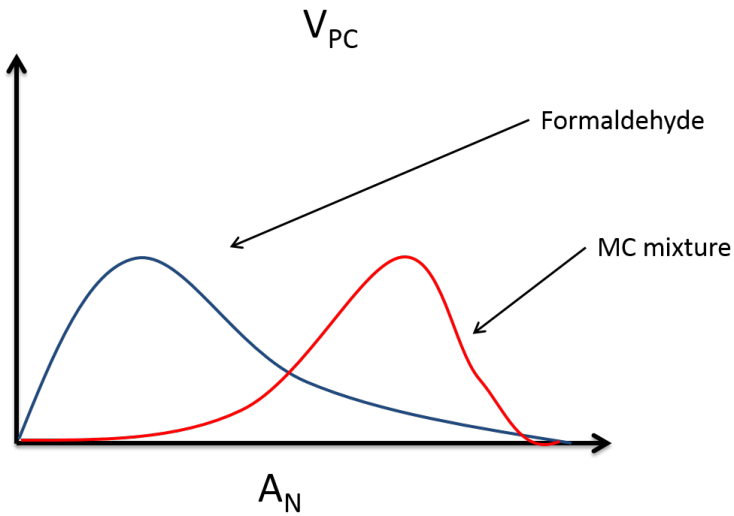

Figure 7.2: Hypothesized model output for the effect of nozzle diameter

- **Main Chamber Ignition:** The interaction of the pre-chamber jets and main chamber charge is least understood. The best approach is optical diagnostics using active laser diagnostic techniques like Laser Induced Fluorescence (LIF) to understand the effect of fuel rich combustion in the pre-chamber (and also the inhomogeneity of the mixture inside the pre-chamber) on the concentration of active species ejected in the main chamber, and their effect on the main chamber ignition. Ignition by transient jets are important in several other applications like explosion protection [61] and perhaps the fundamental mechanism of ignition by pre-chamber jets bears some resemblance.

Bibliography

[1] IPCC, 2014: Climate Change 2014: Synthesis Report. Contribution of Working Groups I, II and III to the Fifth Assessment Report of the Intergovernmental Panel on Climate Change [Core Writing Team, R.K. Pachauri and L.A. Meyer (eds.)]. IPCC, Geneva, Switzerland, 151 pp.

[2] Annual European Union greenhouse gas inventory 1990-2011 and inventory report 2013, Technical report No. 8/2013, European Environment Agency, 2013.

[3] 'Inventory of U.S. Greenhouse Gas Emissions and Sinks: 1990-2013', The U.S. Environmental Protection Agency Report No. EPA 430-R-15-004, 2015.

[4] 'How nitrogen oxides affect the way we live and breathe', The U.S. Environmental Protection Agency Report No. EPA 456/F-98-005, 1998.

[5] P. Wolkoff, C. K. Wilkins, P. A. Clausen, and G. D. Nielsen. Organic compounds in office environments sensory irritation, odor, measurements and the role of reactive chemistry. *Indoor Air*, 16(1):7–19, 2006.

[6] Stanley T. Omaye. Metabolic modulation of carbon monoxide toxicity. *Toxicology*, 180(2):139 – 150, 2002.

[7] P. Tikuisis, D. M. Kane, T. M. McLellan, F. Buick, and S. M. Fairburn. Rate of formation of carboxyhemoglobin in exercising humans exposed to carbon monoxide. *Journal of Applied Physiology*, 72(4):1311–1319, 1992.

[8] Ole et al. Raaschou-Nielsen. Air pollution and lung cancer incidence in 17 european cohorts: prospective analyses from the european study of cohorts for air pollution effects (escape). *The Lancet Oncology*, 14(9):813–822, 2013.

[9] IARC: diesel engine exhaust carcinogenic, International Agency for Research on Cancer, Press Release No. 213, 12th June, 2012.

[10] Clean Power for Transport: A European alternative fuels strategy, European Commission com (2013) 17, 24/1/2013.

[11] Data cource: US Energy Information Administration (2013).

[12] 'Well-to-wheels analysis of future automotive fuels and powertrains in the European context', European Commission Joint Research Centre, Institute for Energy, WELL-to-WHEELS Report Version 3c, July 2011.

[13] J.D. Dale, M.D. Checkel, and P.R. Smy. Application of high energy ignition systems to engines. *Progress in Energy and Combustion Science*, 23(56):379 – 398, 1997.

[14] Smy P. Dale, J. and R. Clements. Laser ignited internal combustion engine - an experimental study. SAE Technical Paper 780329, 1978. doi:10.4271/780329.

[15] Richardson S. Woodruff S. McMillian, M. and D. McIntyre. Laser-spark ignition testing in a natural gas-fueled single-cylinder engine. SAE Technical Paper 2004-01-0980, 2004. doi:10.4271/2004-01-0980.

[16] Karim GA. combustion in Gas Fueled Compression: Ignition Engines of the Dual Fuel Type. ASME. J. Eng. Gas Turbines Power. 2003;125(3):827-836. doi:10.1115/1.1581894.

[17] Ghazi A. Karim. A review of combustion processes in the dual fuel enginethe gas diesel engine. *Progress in Energy and Combustion Science*, 6(3):277 – 285, 1980.

[18] Schock H. Toulson, E. and W. Attard. A review of pre-chamber initiated jet ignition combustion systems. SAE Technical Paper 2010-01-2263, 2010. doi:10.4271/2010-01-2263.

[19] 'Volvo Trucks declares itself first manufacturer of efficient Dual-fuel Euro V Engine, NGV Global news December 15, 2009.

[20] Information on Gas fired engines from company website, http://www.wartsila.com, retrieved on 25/10/2013.

[21] Information on Gas fired engines from company website, http://www.man.com, retrieved on 25/10/2013.

[22] Lyle Cummins. *Internal Fire: The Internal Combustion Engine 1673-1900.* Carnot Press, 2002.

[23] N. A. Otto. Improvement in gas-motor engines. US Patent 194,047, 1877.

[24] Harry Ralph Ricardo. Internal-combusiton engine. US Patent 1,271,942, 1918.

[25] Caleb E. Summers. Internal-combusiton engine. US Patent 1,568,638, 1926.

[26] Marion Mallory. Internal-combusiton engine. US Patent 2,121,920, 1937.

[27] Albert Bagnulo. Internal combusiton engine fed with heavy fuels. US Patent 2,065,419, 1933.

[28] Albert Bagnulo. Engine with stratified mixture. US Patent 2,422,610, 1938.

[29] Neil O. Broderson. Method of operating internal-combustion engines. US Patent 2,615,437, 1952.

[30] Ralph M. Heintz. Internal combustion engine. US Patent 2,884,913, 1959.

[31] Goossak Lev Abramovich. Method of prechamber-torch ignition in internal combustion engines. US Patent 3,230,939, 1966.

[32] Gussak, L., Turkish, M., and Siegla D. High chemical activity of incomplete combustion products and a method of prechamber torch ignition for avalanche activation of combustion in internal combustion engines. SAE Technical Paper 750890, 1975. doi:10.4271/750890.

[33] Gussak L. The role of chemical activity and turbulence intensity in prechamber-torch organization of combustion of a stationary flow of a fuel-air mixture. SAE Technical Paper 830592, 1983. doi:10.4271/830592.

[34] Henry K. Newhall and Ibrabim A. El-Messiri. A combustion chamber concept for control of engine exhaust air pollutant emissions. *Combustion and Flame*, 14(1):155 – 158, 1970.

[35] T. Ken Garrett. Porsche stratified charge engine. *Environmental Science & Technology*, 9(9):826–830, 1975.

[36] W.R. Brandstetter and G. Decker. Fundamental studies on the volkswagen stratified charge combustion process. *Combustion and Flame*, 25:15 – 23, 1975.

[37] Goossak Lev Abramovich. Pulsed jet combustion generator for premixed charge engines. US Patent 4,926,818, 1989.

[38] J.A. Maxson and A.K. Oppenheim. Pulsed jet combustionkey to a refinement of the stratified charge concept. *Symposium (International) on Combustion*, 23(1):1041 – 1046, 1991. Twenty-Third Symposium (International) on Combustion.

[39] Eiichi Murase, Shinsuke Ono, Kunihiko Hanada, Jyong Ho Yun, and Antoni K. Oppenheim. Performance of pulsed combustion jet at high pressures and temperatures. {*JSAE*} *Review*, 17(3):245 – 250, 1996.

[40] Wolanski, P., Dabkowski, A., and Przastek J. Influence of pjc ignition on efficiency and emission of ic piston engine operating at partial and full load. SAE Technical Paper 972871, 1997. doi:10.4271/972871.

[41] David L. Reuss Paul M. Najt, Rodney Brewer Rask. Dual mode engine combustion process. US Patent 6,595,181, 2003.

[42] David Cook Jasim Ahmed Aleksandar Kojic, Jean-Pierre Hathout. Control of auto-ignition timing for combustion in piston engines by prechamber compression ignition. US Patent 6,953,020, 2005.

[43] Pape-J. Gruenig C. Kuhnert D. Getzlaff, J. Investigations on pre-chamber spark plug with pilot injection. SAE Technical Paper 2007-01-0479, 2007. doi:10.4271/2007-01-0479.

[44] William Attard. Turbulent jet ignition pre-chamber combustion system for spark ignition engines. US Patent 2012/0103302, 2012.

[45] Kohn-J. Attard, W. and P. Parsons. Ignition energy development for a spark initiated combustion system capable of high load, high efficiency and near zero nox emissions. SAE Int. J. Engines 3(2):481-496, 2010. doi:10.4271/2010-32-0088.

[46] Fraser-N. Parsons P. Attard, W. and E. Toulson. A turbulent jet ignition pre-chamber combustion system for large fuel economy improvements in a modern vehicle powertrain. SAE Int. J. Engines 3(2):20-37, 2010. doi:10.4271/2010-01-1457.

[47] P. Einewall and B. Johansson. Combustion chambers for supercharged natural gas engines. SAE Technical Paper 970221, 1997. doi:10.4271/970221.

[48] Toulson, E., Schock, H., and Attard W. A Review of Pre-Chamber Initiated Jet Ignition Combustion Systems. SAE Technical Paper 2010-01-2263, 2010. doi:10.4271/2010-01-2263.

[49] Gussak, L., Karpov, V., and Tikhonov Y. The application of lag-process in prechamber engines. SAE Technical Paper 790692, 1979. doi:10.4271/790692.

[50] John B Heywood. *Internal combustion engine fundamentals*. Mcgraw-hill New York, 1988.

[51] G. Woschni. A universally applicable equation for the instantaneous heat transfer coefficient in the internal combustion engine. SAE Technical Paper 670931, 1967. doi:10.4271/670931.

[52] Nielsen-L. Eriksson, L. and J. Nytomt. Ignition control by ionization current interpretation. SAE Technical Paper 960045, 1996. doi:10.4271/960045.

[53] Y. Cao and L. Li. A novel closed loop control based on ionization current in combustion cycle at cold start in a gdi engine. SAE Technical Paper 2012-01-1339, 2012. doi:10.4271/2012-01-1339.

[54] G. Malaczynski and M. Baker. Real-time digital signal processing of ionization current for engine diagnostic and control. SAE Technical Paper 2003-01-1119, 2003. doi:10.4271/2003-01-1119.

[55] Roethlisberger, R., and Favrat D. Investigation of the prechamber geometrical configuration of a natural gas spark ignition engine for cogeneration: part i. numerical simulation. *International Journal of Thermal Sciences*, 42(3):223–237, 2003. doi:10.1016/S1290-0729(02)00023-6.

[56] Yagi-S. Ishizuya A. Date, T. and I. Fujii. Research and development of the honda cvcc engine. SAE Technical Paper 740605, 2003. doi:10.4271/740605.

[57] ENGVA position paper on Euro-VI emission limits in relation to heavy-duty natural gas vehicles. European Natural Gas Vehicle Association, Updated version, 2007.

[58] ANSYS® Fluent®, Release 15.0, Theory Guide, 4.3.3. Realizable k-ϵ Model, ANSYS, Inc.

[59] Gi-Heon Kim Allan Kirkpatrick and Daniel Olsen. Cfd modeling of the performance of a prechamber for use in a large bore natural gas engine. Paper No. ICES2005-1049 in the Proceedings of ICES2005 - ASME Internal Combustion Engine Division 2005 Spring Technical Conference, April 5-7, 2005, Chicago, IL, USA, 2014.

[60] D Favrat S Heyne, G Millot. Numerical simulations of a prechamber autoignition engine operating on natural gas. *International Journal of Thermodynamics (IJoT)*, 14(2):43–50, 2011. doi:10.5541/ijot.166.

[61] A. Ghorbani, G. Steinhilber, D. Markus, and U. Maas. Ignition by transient hot turbulent jets: An investigation of ignition mechanisms by means of a pdf/redim method. *Proceedings of the Combustion Institute*, 35(2):2191 – 2198, 2015.